



Democratic and Popular Republic of Algeria
Ministry of Higher Education and Scientific Research

Mohamed Khider University of Biskra
Faculty of Exact Sciences, Natural and Life Sciences
Department of Science Material

Master Dissertation

Field: Science Material
Option : Chemistry
Specialty : Pharmaceutical Chemistry

Ref. :

Submitted by:
Chahbaoui Narimene

September 2020

Élaboration et caractérisation chimique d'un biomatériau de substitution osseuse

Board of Examiners:

Dr	Boussehel Hamida	MCB	Med Khider University Biskra	President
Dr	Kribaa Oum Keltoum	MCA	Med Khider University Biskra	Supervisor
Dr	Djoudi Lynda	MCB	Med Khider University Biskra	Examiner

Academic year: 2019/2020

Acknowledgments

First and foremost, I thank Allah, the Almighty, for giving me the strength and patience to carry on this project and for blessing me with many great people who have been my greatest support in my academic life.

My sincere gratitude and appreciation go to my supervisor, **Dr. Kribaa Oum Keltoum**, for the opportunity of working in the fascinating world of biomaterials, for her unwavering support, encouragement and guidance throughout the course of my work.

My gratitude goes also to the members of the jury: **Dr. Boussahel Hamida** and **Dr. Djoudi Linda**, who accepted to examine and evaluate my work.

I would also extend my thanks to all the laboratory staff of chemistry, from our SM department, especially: Ms. Farhi D. for her kindness, support and for providing me with the material resources I needed to carry out this research work.

My last thanks go to my beautiful family. There are no words to express how much I am grateful to them for the invaluable support, unconditional love and encouragement, Special thanks to parents that I adore, for everything they do for me. I am very proud for being their daughter and to take part in their lives. Thanks for the strength, courage and determination they pass me and for never let me give up of my dreams.

Abstract

Hydroxyapatite, $\text{Ca}_{10}(\text{PO}_4)_6(\text{OH})_2$, like other related calcium phosphate minerals, has been used extensively as an orthopedic implant material for many years due to its excellent biocompatibility, bone bonding ability and also due to its structural and compositional similarity to that of the mineral phase of hard tissue in human bones. Therefore, in this study, HA was synthesized using calcium hydroxide $\text{Ca}(\text{OH})_2$ and di-ammonium hydrogen phosphate $(\text{NH}_4)_2\text{HPO}_4$ as calcium and phosphate precursors, respectively. The hydroxyapatite powders were characterized by X-ray diffraction (XRD), Fourier transform infrared (FTIR) spectroscopy, and scanning electron microscope (SEM) in conjunction with energy dispersive x-ray spectroscopy (EDX) to provide information about crystal structure, composition, functional group distribution, and morphology.

Keywords : bone substitutes, calcium phosphate, hydroxyapatite.

Résumé

Hydroxyapatite, $\text{Ca}_{10}(\text{PO}_4)_6(\text{OH})_2$, comme d'autres minéraux de phosphate de calcium, a été largement utilisé comme matériau d'implant orthopédique pendant de nombreuses années en raison de son excellente biocompatibilité, sa capacité de liaison osseuse et également en raison de sa similarité structurelle et compositionnel avec celle de la phase minérale des tissus durs des os humain. Par conséquent, dans cette étude, HA a été synthétisé en utilisant l'hydroxyde de calcium $\text{Ca}(\text{OH})_2$ et le phosphate de diammonium $(\text{NH}_4)_2\text{HPO}_4$ comme précurseurs de calcium et de phosphore, respectivement. Les poudres d'hydroxyapatite ont été caractérisées par diffraction des rayons X (DRX), spectroscopie infrarouge à transformée de Fourier (FTIR), et microscopie électronique à balayage (MEB) couplée avec spectroscopie de rayons X à dispersion d'énergie (EDX) pour fournir des informations sur la structure cristalline, la composition, la distribution de groupe fonctionnelle et la morphologie.

Mots-clés : substituts osseux, phosphate de calcium, hydroxyapatite.

ملخص

هيدروكسي أباتيت؛ $Ca_{10}(PO_4)_6(OH)_2$ ؛ مثل معادن فوسفات الكالسيوم الأخرى؛ تم استخدامه بشكل مكثف كمادة لزراعة العظام لسنوات عديدة نظرًا لتوافقه الحيوي الممتاز وقدرته على الترابط العظمي وأيضًا بسبب تشابهه الهيكلي والتركيب مع المعادن المكونة للأنسجة الصلبة في عظام الإنسان. لذلك، في هذه الدراسة، تم تصنيع *HA* باستخدام هيدروكسيد الكالسيوم $Ca(OH)_2$ وثنائي فوسفات الأمونيوم $(NH_4)_2HPO_4$ كسلائف الكالسيوم والفوسفات، على التوالي. تم الكشف على مساحيق هيدروكسي أباتيت بإستعمال إنعراج الأشعة السينية (*XRD*)، التحليل الطيفي للأشعة تحت الحمراء (*FTIR*)، ومجهر المسح الإلكتروني (*SEM*) بالتزامن مع التحليل الطيفي للأشعة السينية المشتتة للطاقة (*EDX*) لتوفير معلومات حول البنية البلورية؛ التركيب؛ توزيع المجموعات الوظيفية والمورفولوجيا.

الكلمات المفتاحية: بدائل العظام، فوسفات الكالسيوم، هيدروكسي أباتيت.

Glossary

Words labelled with an asterisk (*) in the manuscript are defined in this glossary.

Allograft: a tissue graft from a donor of the same species as the recipient but not genetically identical.

Autograft: a tissue graft from one point to another of the same individual's body.

Biocompatibility: the capability of coexistence with living tissues or organisms without being toxic, injurious, or physiologically reactive and not causing immunological rejection.

Bone marrow: the fatty network of connective tissue that fills the cavities of bones.

Canaliculi: is a small channel in ossified bone.

Lamellae: a thin plate-like structure, often one amongst many lamellae very close to one another, with open space between.

Mesenchymal cells: refers to cells that develop into connective tissue, blood vessels, and lymphatic tissue.

Mineralization: the process by which the organic bone matrix becomes filled with calcium phosphate nanocrystals.

Osteoconduction: the process by which bone grows on a surface.

Osteoconductive: relating to osteoconduction.

Osteoinduction: osteoinductive materials stimulate mesenchymal stem cells along the osteoblastic pathway and lead these cells in the formation of new bone.

Osteoinductive: relating to osteoinduction.

Osteoporosis: a medical condition in which the bones become brittle and fragile from loss of tissue, typically as a result of hormonal changes, or deficiency of calcium or vitamin D.

Plasma spraying: it is a coating processes in which melted (or heated) materials are sprayed onto a surface.

List of figures

Figure 1.1-1 Schematic drawing of bone.....	4
Figure 1.1-2 Schematic drawing of collagen fibers and apatite crystals.....	4
Figure 1.2-1 Bone remodeling process showing the coordinated action of osteoclasts and osteoblasts.....	6
Figure 1.2-2 Bone healing schema illustrating the phases of the process: reactive (a), reparative (b, c), and remodeling (d).....	7
Figure 1.6-1 Bioactivity spectrum for various bioceramic implants.....	15
Figure 2.3-1 Crystal structure of hydroxyapatite.....	20
Figure 2.5-1 Illustration of the head-to-toe clinical uses of HA.....	27
Figure 3.1-1 Schematic representation of the preparation steps of HA.....	28
Figure 3.1-2 Flow chart of the synthesis of Hydroxyapatite.....	29
Figure 3.2-1 Illustration of Bragg's Law for constructive interference.....	31
Figure 3.2-2 Shimadzu FTIR: 8400S.....	32
Figure 3.2-3 Scanning Electron Microscope JEOL JSM-6390LV.....	33
Figure 4.1-1 XRD pattern of HA heat-treated at 200°C.....	35
Figure 4.1-2 XRD pattern of HA heat-treated at 500°C.....	35
Figure 4.1-3 XRD pattern of HA heat-treated at 600°C.....	36
Figure 4.1-4 XRD patterns of synthetic and natural HA.....	36
Figure 4.2-1 FTIR spectrum of HA at 100°C.....	37
Figure 4.2-2 FTIR spectrum of HA at 200°C.....	38
Figure 4.3-1 EDX pattern of synthetic HA calcined at 800°C.....	38
Figure 4.3-2 EDX Pattern of natural HA extracted from bovine bone calcined at 800°C.....	39
Figure 4.4-1 SEM image of synthetic HA at 200°C.....	39
Figure 4.4-2 SEM image of synthetic HA at 800°C.....	40
Figure 4.4-3 SEM image of natural HA extracted from bovine bone at 800°C.....	40

List of tables

Table 1.1-1	Mechanical properties of human bone	5
Table 1.5-1	Materials for use in the body	10
Table 1.6-1	Classification schema for bioceramics	14
Table 2.1-1	Family of calcium phosphate compounds	17
Table 2.2-1	Composition of biological apatites and hydroxyapatite	18
Table 2.2-2	Properties of biological apatites and hydroxyapatite	19
Table 2.3-1	Advantages and disadvantages of some of the synthesis methods for HA	25

Contents

Acknowledgments	i
Abstract	ii
Résumé	iii
ملخص	iv
Glossary	v
List of figures	vi
List of tables	vii
Contents	viii
Introduction	1
References	
Part one: Literature review	
Chapter one: Biomaterials for bone regeneration	
1.1 Bone structure and functions	3
1.2 Bone remodeling and healing	6
1.3 Bone deficiency, clinical needs, and current treatments	8
1.4 Critical analysis of the literature	9
1.5 Biomaterials	9
1.5.1 Bioinert materials	11
1.5.2 Bioactive materials	12
1.5.3 Bioresorbable materials.....	13
1.6 Bioceramics	14
References	
Chapter two: Hydroxyapatite	
2.1 Calcium phosphate bioceramics	17

2.2	Biological apatites	18
2.2.1	Composition and structure	18
2.2.2	Properties	19
2.3	Hydroxyapatite	19
2.3.1	Structure	19
2.3.2	Thermal properties of HA	21
2.3.3	Synthesis of HA	23
2.4	HA production method from biogenic resources	26
2.5	Clinical application of HA	26
References		
Part two: Experimental study		
Chapter three: Materials & methods		
3.1	Synthesis of Hydroxyapatite	28
3.1.1	Materials	28
3.1.2	Experimental procedure	28
3.2	Characterization methods	30
3.2.1	X-Ray Diffraction	30
3.2.2	Fourier Transform Infrared Spectroscopy	31
3.2.3	Scanning Electron Microscopy & Energy Dispersive Analysis of X-ray	32
References		
Chapter four: Results & discussion		
4.1	X-ray Diffraction analysis	34
4.2	Fourier Transform Infrared Spectroscopy (FTIR).....	37
4.3	Energy Dispersive X-Ray Analysis	38
4.4	Scanning Electron Microscopy	39
Conclusion & future work		41
Appendix		43

Introduction

Biomaterials have been gaining increasing interest due to their applicability to aging populations and the treatment of diseases. Research on developing new biomaterials or manipulating the structure and composition of existing ones has been intensively directed on improving the biomedical device's properties. Biomaterials act to restore, repair, or replace the damaged tissue by integrating with the body's problematic part to increase the life expectancy. The different mechanical, physical, chemical, and structural properties of biomaterials allow them to be used in various applications depending on their biocompatibility* and characteristics. In general, biomaterials are used as implants, tissues, organ transplants, and drug delivery systems [1].

Ceramics are a class of biomaterials widely used as implant materials due to their ability to be fabricated into various shapes with high compressive strength, variable porosity, and bioactive properties in the body. The significant similarity in the chemical composition of some ceramics, such as calcium phosphate with human bone minerals makes them suitable for orthopedic implants, and dental materials [2]. These materials show excellent bioactivity, high biocompatibility, and unique osteoconduction* characteristics [3].

Hydroxyapatite with the chemical formula $\text{Ca}_{10}(\text{PO}_4)_6(\text{OH})_2$, is thermodynamically stable in its crystalline state in body fluid and has a very similar composition to bone mineral [1]. HA can integrate with bone without causing any local or systemic toxicity, inflammation, or foreign body response. For these reasons, HA has been widely used for biomedical applications, particularly in orthopedic, odontology, and coating material for metallic implants [5].

The objective of this work is thus to synthesize hydroxyapatite and study the influence of the thermal treatment on the structure and morphology of the obtained powder.

The manuscript is organized in two parts: “Literature review” and “Experimental study”.

The first part is split into two chapters:

- The first chapter discusses the basic knowledge of human bone structure, composition, and properties needed to understand the requirements of a biomaterial destined for orthopedic implants. This is followed by a glimpse at the current bone substitute materials and their applications, the need for synthetic alternatives, and details of the different types of biomaterials based on their host response with special consideration of bioceramics.
- The second chapter starts with emphasizing the structure of hydroxyapatite, its main properties with the various methods of synthesis, and ends with some of HA applications in the medical field.

The second part is also divided into two chapters:

- Chapter three outlines the process adopted to synthesize the HA in this study along with the methods and apparatus used to characterize the produced materials.
- Chapter four presents the results obtained and an analysis of these findings.

Finally, the manuscript ends with general conclusions and future work.

References

- [1] M. Sadat-Shojai, M. Khorasani, E. Dinpanah-Khoshdargi and A. Jamshidi, "Synthesis methods for nanosized hydroxyapatite in diverse structures," *Acta Biomaterialia*, vol. 9, no. 8, pp. 7591-7621, 2013.
- [2] G. M. Raghavendra, K. Varaprasad and T. Jayaramudu, "Biomaterials," *Nanotechnology Applications for Tissue Engineering*, pp. 21-44, 2015.
- [3] N. Lertcumfu, P. Jaita, S. Manotham and al, "Properties of calcium phosphates ceramic composites derived from natural materials," *Ceramics International*, vol. 42, no. 9, pp. 10638-10644, 2016.
- [4] H. R. Rezaie, L. Bakhtiari and A. Öchsner, *Biomaterials and their applications*, Cham: Springer, 2015.
- [5] B. D. Ratner, A. S. Hoffman, F. J. Schoen and J. E. Lemons, *Biomaterials Science: An Introduction to Materials in Medicine*, Elsevier Academic Press , 2004.

Part One

Literature Review

Chapter One

Biomaterials for bone regeneration

To understand bone replacement material requirements, one must understand bone histology, structure, and biology, in addition to the factors that govern and affect the remodeling and healing of bone. This Chapter reviews these properties from the perspective of a material scientist. Factors that are relevant to the incorporation of bone into a bioceramic graft material are of primary importance from this aspect, and therefore this is where the focus lies.

1.1 Bone structure and functions

Bone is an extremely complex tissue that performs many essential functions in the body and is complicated to analyze because it has so many levels of organization. Bone has numerous primary functions in the body as a system, such as:

- protection of vital organs, e.g., the rib cage protects the heart and lungs;
- providing support and site of muscle attachment for locomotion;
- generation of red and white blood cells for immunoprotection and oxygenation of other tissues;
- retaining reserve stores of calcium, phosphate, and other essential ions [1].

Bone is a biological composite comprising 90 % extracellular matrix (ECM) and 10 % water [2]. The ECM is composed of 60 – 70 % inorganic mineral, usually referred to as hydroxyapatite (HA), which has a similar, but not identical structure to natural bone mineral.

HA has a chemical formula of $\text{Ca}_{10}(\text{PO}_4)_6(\text{OH})_2$ and calcium-phosphorus (Ca:P) ratio of 5:3 (1.67). Bone apatite is considered to be a carbonate apatite called *dahlite* that is held to resemble an octacalcium crystal that naturally forms in plates. It is characterized by calcium, phosphate, and hydroxyl deficiency with typical Ca:P ratios between 1.37 and 1.87 [3]. The remaining 20 – 30 % of bone ECM contains organic components composed of type I collagen (90 %) with noncollagenous proteins, e.g., glycosaminoglycans constituting the remainder. The collagen confers flexibility and fractures toughness to the matrix, and the inorganic phase confers stiffness.

Macroscopically there are two types of bone, cortical and cancellous (Figure 1.1-1). Cortical bones represent 80 % of skeletal tissue, also known as compact bone, has a dense structure with a high load-bearing ability and form the outer layer of the bone tissue. Cancellous bone comprises the bone center, also known as spongy bone, has a high surface area, and houses the bone marrow*. This bone has a lower density compared to cortical bone and provides metabolic functions for the bone.

Bone has different layers and microstructure that cannot be seen with naked eyes, like Haversian canals, which hold the blood vessels, lamellae*, osteons, and canaliculi*. The major component of both cortical and trabecular bone are osteons, and within them, we find Haversian canals. These canals are cylindrical and contain blood vessels to nourish the tissue. The

concentric lamellae matrix forms the walls of the canals. Osteons represent the nanoscale structure of the bone and are composed of collagen fibers/fibrils, which house mineral crystals in gaps between them (Figure 1.1-2) [4,5].

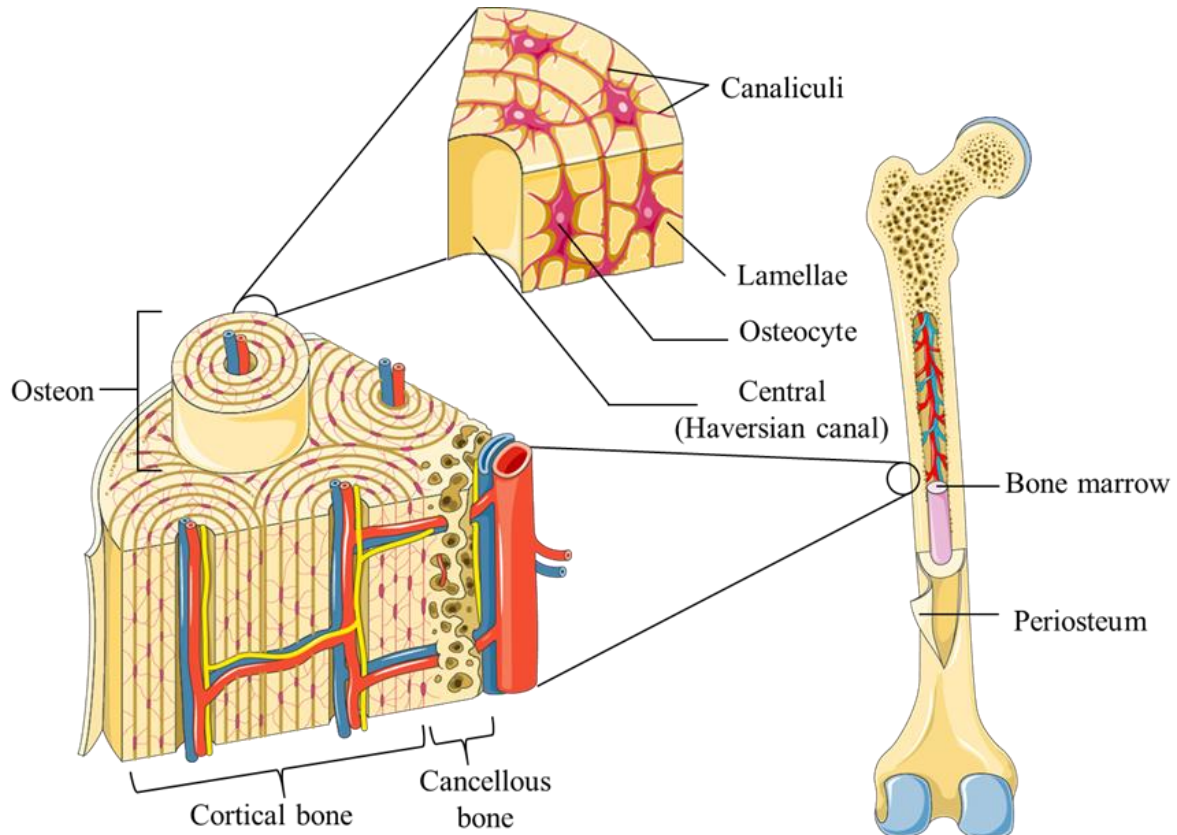


Figure 1.1-1 Schematic drawing of bone. Adapted from [14]

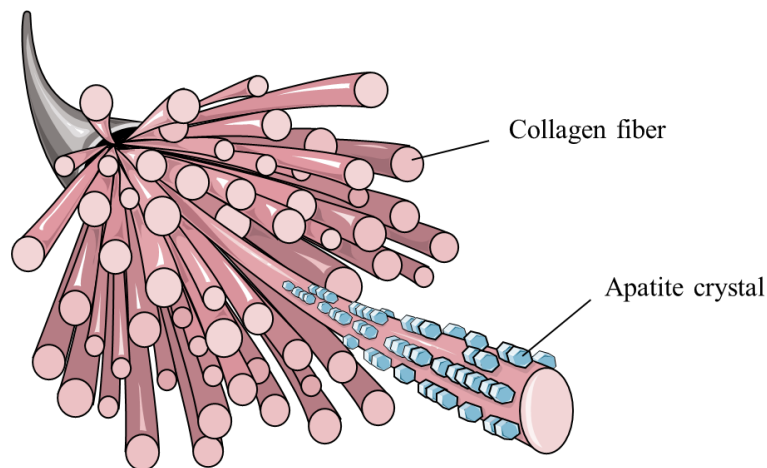


Figure 1.1-2 Schematic drawing of collagen fibers and apatite crystals. Adapted from [14]

A summary of the mechanical properties of bone is shown in Table 1.1-1. It is vital to match the bone graft strength with the natural bone to prevent failure to improper stiffness or flexibility, before any bone replacement surgery.

Table 1.1-1 Mechanical properties of human bone. Adapted from [7,8]

Property	Cortical bone	Cancellous bone
Tensile strength (MPa)	50-150	10-100
Compressive strength (MPa)	130-230	2-12
Young's modulus (GPa)	7-30	0.02-0.5
Strain to failure (%)	1-3	5-7
Shear strength (MPa)		53-70
Shear modulus (GPa)		3

Bone consists of five distinct types of living cells: osteoprogenitor cells, osteoblasts, osteocytes, osteoclasts, and bone-lining cells. Bone, like other connective tissues in the embryo, is derived from mesenchymal cells*. These cells can divide and differentiate into bone cells, which are known as osteoprogenitor cells, also known as bone-precursor cells.

Osteoblasts are the cells responsible for the formation of new bone. They start with secreting collagen and then coat it with noncollagenous proteins, which is similar to glue, that can hold the minerals, mostly calcium and phosphate from the bloodstream, leading to new bone formation. Osteocytes are mature cells derived from osteoblasts, which are responsible for the maintenance of bone. They function as transporting agents of minerals between bone and blood. Osteoclasts are the giant cells found at the surface of the bone mineral next to the resorbing site. They are responsible for the resorption of the bone. They use acids or enzymes to dissolve the minerals as well as collagen from the matured bone. The dissolved minerals then re-enter the bloodstream and are carried to different parts of the body when needed. Bone-lining cells are found along with the surface of the matured bone; they are responsible for regulating the transportation of minerals in and out of the bone tissue. They also respond to hormones by making some exclusive proteins that activate the osteoclasts.

These five types of cells are responsible for building the bone matrix with hierarchical self-assembly, maintenance, and remodeling as required. All these processes must be in equilibrium to ensure a healthy bone [9].

1.2 Bone remodeling and healing

Bone is a very dynamic tissue, which undergoes constant remodeling throughout the lifetime and displays regeneration properties after injury. Remodeling is the result of the complex interplay between osteoclasts and osteoblasts, which secure bone resorption and deposition, respectively [10]. It is regulated by the coordinated action of different biochemical and biophysical stimuli. The process of remodeling mainly occurs to repair small bone fractures and is required for the maintenance of a normal healthy bone, as well as for adaptation to external stress and loading [11].

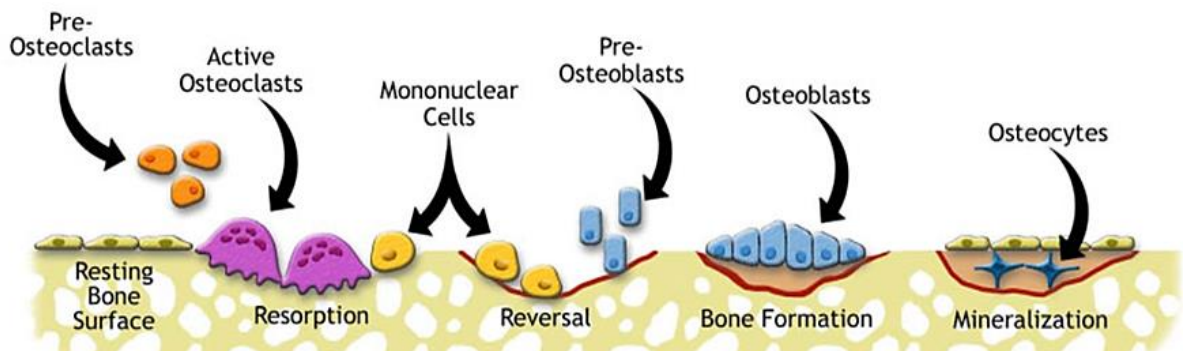


Figure 1.2-1 Bone remodeling process showing the coordinated action of osteoclasts and osteoblasts. Adapted from [38]

As a result of remodeling, about 5% of cortical bone and 20% of trabecular bone are renewed every year. Unbalanced bone formation/resorption activity is associated with bone-weakening [12] and is considered to be a major cause leading to osteoporosis* [13]. Figure 1.2-1 presents a schematic illustration of the bone remodeling process. At first, pre-osteoclasts are attracted to the remodeling sites, become fused, and form multinucleated osteoclasts. During the resorption phase, the osteoclasts dig out a cavity called a resorption pit. As while this pit is being dug out, calcium is released into the blood for use in various body functions. The resorption phase ends with the disappearing of osteoclasts. In the reversal phase, mesenchymal stem cells appear along with the remodeling site and begin to increase in number and become specialized into pre-osteoblasts. During the formation phase, the pre-osteoblasts mature into osteoblasts and busy themselves by releasing collagen and absorbing calcium and phosphorus from the blood and depositing it in the form of hydroxyapatite, thus creating new bone. After that, osteoblasts can be either trapped in this new bone (becoming osteocytes) or flattened on its surface to

become bone lining cells. The remodeling site (now new bone tissue) remains resting/quiescence until the next bone remodeling cycle begins.

Besides the remodeling ability, bone tissue displays an intrinsic capacity to self-heal structural defects after injury. By healing, a fractured or broken bone is repaired in the direction of restoring the physical, mechanical, and functional conditions prevailing before fracture [14]. There are three distinct phases in the process of bone healing: reactive phase, reparative phase, and remodeling phase (Figure 1.2-2).

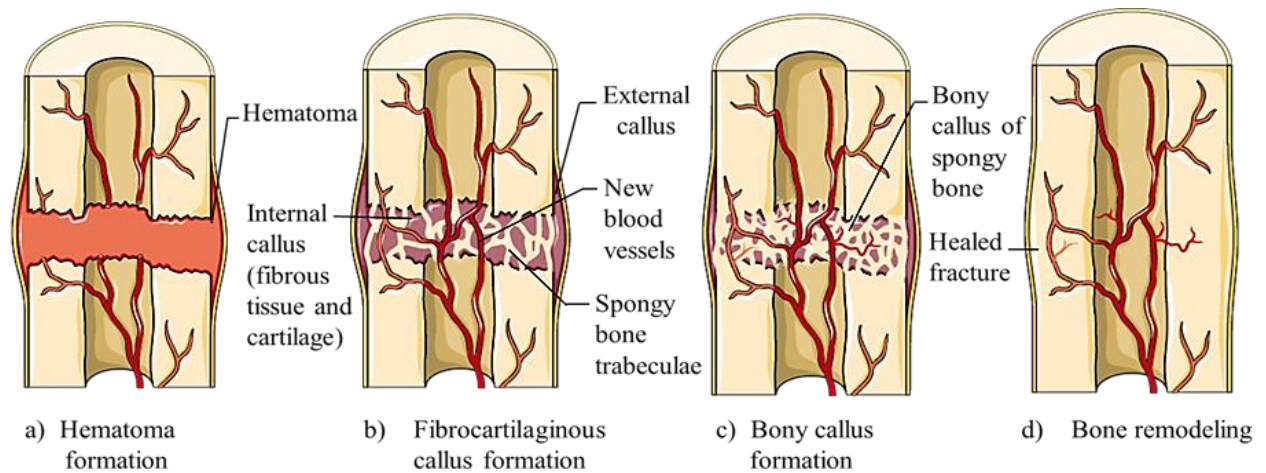


Figure 1.2-2 Bone healing schema illustrating the phases of the process: reactive (a), reparative (b, c), and remodeling (d). Adapted from [14]

- **Reactive phase:** blood vessels are disrupted, leading to bleeding and the formation of a clot. Typically, within 6-8 hours, the clot has formed what is known as a fracture hematoma. This clotting reduces the blood supply to many of the cells in the area of injury, and as a result, these cells die.
- **Reparative phase:** white blood cells are then recruited to remove any dead cells and debris. Fibroblast and osteoblast cells are also recruited, stabilizing the fracture. The fibroblasts form granulation tissue around the broken ends of the bone while the osteoblasts begin to synthesize spongy bone, forming a fibrocartilaginous callus. In the weeks that follow, the fibrocartilaginous callus is replaced by a bony callus known as cancellous bone, and newly formed blood vessels increase.
- **Remodeling phase:** The bony callus then undergoes repeated remodeling. This process relies on a balance of resorption by osteoclasts and new bone formation by osteoblasts. This

step may occur over several months until the bone has returned to its original state, and even after, the bone may remain uneven for years [15].

1.3 Bone deficiency, clinical needs, and current treatments

Despite the intrinsic capacity of bone to regenerate and self-repair, this ability is limited to small fractures, and therapeutic solutions need to be applied to promote bone healing in case of defects of crucial size (delayed union and nonunion fractures). Moreover, bone replacement therapies are required to prevent bone deficiencies associated with reconstruction of congenital and traumatic skeletal defects, cosmetic procedures, degenerative disorders (i.e., osteoporosis), and surgical resection following neoplastic transformation and chronic infection [16]. The worldwide market for bone replacement and repair therapies was estimated to be approximately €300 million in 2003, several bone grafting procedures reaching 2.2 million in 2006 [17]. Today, the number of elderly reporting age-related fractures is estimated to be nearly 100 million per year worldwide, and this number is projected to massively increase over the next decades, with the number of older people (+65 years) estimated to be about 2 billion by 2050. In several clinical cases associated with bone deficiency, patient comfort, and bone functionality can only be restored by surgical reconstruction. Current treatments for these patients are based on the transplantation of autograft, allograft, or bone graft substitute.

Autogenic bone grafts (autograft*) represent the gold standard treatment for bone replacement procedures, due to immune tolerability and provision of essential components supporting bone regeneration and repair, resulting in fast integration and revascularization. However, limited availability and donor site morbidity restrict their use in several clinical cases [18]. On the other hand, allogeneic bone grafts (allograft*), which are usually derived from decellularized (and demineralized) living or cadaveric bone tissue, are available in large amounts but integrate slowly, carry the risk of infection transmission and may display immune incompatibility leading to transplant rejection [19]. Besides their respective advantages, both autograft and allograft lack the potential to provide significantly customized bone substitutes for the exact reconstruction of complex bone defects in particular clinical situations.

This is why synthetic bone grafts substitutes present an attractive alternative to natural bone grafts, in the first place because of their unlimited and off-the-shelf availability. Second, the fact that they do not cause an immunogenic response and that they can easily be tailored to

meet the requirements of a specific application explains a great number of substitutes developed in the past few decades. Although all three material types, metals, polymers, ceramics, and combinations thereof have been used to develop bone graft substitutes, the use of calcium phosphate (CaP)-based biomaterials, mostly ceramics, has granted the most considerable interest. The fact that the inorganic component of bone is a CaP mineral is the main reason for this interest. It emphasizes the fact that the rationale behind a tissue regeneration strategy is often an attempt to create an optimal environment for regeneration [20].

1.4 Critical analysis of the literature

Once the context of this thesis is described, the question of what material system could be suggested as a bone substitute should be posed. Based on the bone composition and structure, bone mechanical properties, and healing, what properties or conditions should a material candidate meet for bone substitution?

A first and basic argument is that nature is in charge of the process of bone remodeling and healing. Cells have the inherent capability for self-organization, to form complex structures, under the appropriate conditions. Therefore, a suitable general property of a bone substitute material is that it does not hinder the natural process but provides a favorable environment for cell function, that is, for cells to live, grow and differentiate and produce their mineralized ECM. On the other hand, bone substitute material should provide physical support for cells and morphology to favor vascularization and the flow of biological fluids. Also, it could be useful that the material provides calcium and phosphate needed in the formation of apatite in the mineralization* process. Once the new bone is formed, the bone substitute material should degrade and be absorbed by the body without any toxicity. In strict terms, the material with potential for bone substitution should be non-toxic, biodegradable, osteoinductive*, osteoconductive*, porous, and mechanically stable. Besides those basic properties, a compromise should be met between sophistication, ease of handling by the surgeon, ease of production, ease of placing on the market, and costs [21].

1.5 Biomaterials

Biomaterials may be defined as:

“A nonviable material used in a medical device, intended to interact with biological systems.”

(1st Biomaterials Consensus Conference, 1986, Chester, UK)

“A material intended to interface with biological systems to evaluate, treat, augment, or replace any tissue, organ, or function of the body.”

(2nd Biomaterials Consensus Conference, 1992, Chester, UK)

The first characteristic of a biomaterial is biocompatibility, i.e., the ability to induce an appropriate response within the human body after implantation. Biomaterials may be metals, ceramics, polymers, and composites, and, according to their composition, they exhibit peculiar properties (Table 1.5-1). For example, metals have good mechanical properties and high toughness. Instead, ceramics generally offer high wear and corrosion resistance, even if they are hard and fragile. According to their interaction with the human body, biomaterials can be “bioinert,” “bioactive,” and “bioresorbable.”

Table 1.5-1 Materials for use in the body. Adapted from [22]

Material	Advantage	Disadvantage	Application
Polymers Nylon PTFE Polyester Silicone	Ductile, light, easy to fabricate	Not strong, prone to creep, degradable	Suture, vascular prosthesis, acetabular cup, artificial ligament
Metals Ti and its alloys Co - Cr alloys Stainless steels: Au, Ag, Pt	Ductile, strong, tough	Prone to corrosion, unwanted ion release	Artificial joint, bone plate, and screw, dental root implant, pacer, suture wire
Ceramics Carbon Aluminum oxide Hydroxyapatite	Biocompatible, Inert or bioactive, strong in compression, stiff	Brittle, weak in tension, sometimes fragile	Cardiovascular device, dental prosthesis, joint prosthesis, orthopedic implant
Composites Carbon-carbon Metal-PMMA HA-HDPE	Strong, stiff, tailor-made, distinctive properties	Difficult to make, high production cost	Joint implant, heart valve, bone cement

1.5.1 Bioinert materials

The first studies on materials for medical applications were designed to find components which could be mechanically strong and chemically inert. For this reason, the first biomaterials, which were introduced in the '20s, were metal alloys, such as Stellite, stainless steel 18-8, and Vitallium. Subsequently, polymers such as PMMA and nylon were applied, with the same goal of using materials that reacted as less as possible with the surrounding environment. A significant advance in the field of biomaterials occurred at the end of World War II. In this period, many veterans required surgery, and hence the attention of the scientific community was driven on the need for new biomaterials; on the other hand, novel durable and inert materials, initially developed for the military applications, had become available [23].

Substantially, the purpose of the first implants was to replace the damaged organ without being rejected. Accordingly, even if no material is completely inert in a biological environment, the first “bioinert” materials aimed to avoid any toxic reaction and to minimize the formation of a non-adherent fibrous capsule at the interface with the host tissue [24].

Nowadays, various kinds of bioinert materials are used, including metal alloys, ceramics such as zirconia and alumina and polymers such as ultra-high molecular weight polyethylene (UHMWPE) and polymethylmethacrylate (PMMA). These materials are chosen mainly because of their mechanical properties. For example, UHMWPE is wear-resistant and possesses self-lubricating properties.

Their tissue-implant interface gives the drawback of the so-called “first generation” biomaterials. Although bioinert materials do not cause adverse reactions by the host tissues, they inevitably get covered by a fibrous capsule when they are implanted in the human body. The capsule is not bonded with the implant, and therefore micro-movements may occur. For this reason, bioinert materials should operate primarily in compression, in order to limit the relative movements between the implant and host tissue, which may deteriorate the functionality of the prosthesis or the original tissue properties at the interface or both. Various methods have been proposed to increase the adhesion between bioinert materials and living tissues. For example, it is possible to modify the surface morphology of the implant: the so-called biological and morphological fixations are obtained using this procedure. The former is achieved when the bone grows within the open porosity of the implant; the ingrowth leads to a mechanical connection of the bone to the biomedical device. The latter occurs when the growing bone

attaches into the superficial irregularities of the implant, and it can be enhanced by increasing the roughness or making fenestration. Among these methods, the biological fixation can ensure the best fixation, but it requires the use of porous materials, which may be mechanically inadequate [23,25].

An alternative solution is cementation, which consists of the fixation of the prosthesis with a polymeric or ceramic cementing paste [26].

1.5.2 Bioactive materials

The second generation of biomaterials was born at the end of the '60s when professor L. L. Hench proposed a new group of glasses able to bond with the bone, the so-called “bioglasses.” [27]. The study of these new materials stemmed from a specific request: a material that could survive the exposure to the human body without any adverse reactions. In fact, at that time, the problem of rejection was still unresolved. So, professor Hench began to study new materials for medical applications based on a hypothesis:

“The human body rejects metallic and synthetic polymeric materials by forming scar tissue because living tissues are not composed of such materials. Bone contains a hydrated calcium phosphate component, hydroxyapatite [HA]. Therefore, if the material can form a HA layer in vivo, it may not be rejected by the body.”

In 1971 the first paper about bioglass was published [28]. The biomaterials of the second generation, commonly called “bioactive materials,” can bond with the host tissue. In particular, when a bioactive glass is implanted, it induces the formation of a superficial layer of hydroxy-carbonate apatite (HCA). The HCA is very similar to the mineral component of bones, and therefore the implant is not perceived as a foreign body. Accordingly, bioactive materials are not covered by a fibrous capsule, as occurs to bioinert materials, but their surface directly bonds to the new host tissues. The result is a strong adhesion between the implanted material and the living tissues, which drastically reduces the problems of rejection and relative micro-movements between the prosthesis and the host tissue. This mechanism is known as “bioactive fixation.” After a few months, the bond between bones and bioactive materials reaches a strength comparable to that of bone. Moreover, some specific bioactive materials can also bond with the collagen of soft tissues [25].

The bioactivity of a material can be assessed in different ways. The most effective one indeed relies upon *vivo* tests, namely experimentation on living organisms. Unfortunately, such tests involve risks to the patient and raise moral problems when they are run on animal models. *In vitro* methods, which mimic specific biological phenomena in an artificial laboratory environment, are most commonly used to assess the bioactivity of new materials. However, *in vitro*, tests are not able to reproduce the complexity of living organisms, and hence they remain preliminary trials. In fact, *in vivo* tests are generally performed on materials that have already been extensively tested *in vitro*. A relatively straightforward approach to test materials *in vitro* consists of soaking them in a simulated body fluid (SBF) [29].

SBF is an acellular fluid that has the same ionic composition of human plasma. These tests are carried out by soaking the sample into a fixed volume of SBF for a specified period under controlled conditions. The purpose is to verify the ability of the biomaterial to develop HCA on its surface. The significance of SBF tests is still under debate due to their intrinsic limits, such as the inability to verify antibody's reactions [30]. Nevertheless, SBF tests remain the principal mean to acquire a preliminary insight into the bioactivity of new materials.

1.5.3 Bioresorbable materials

Bioresorbable materials are gradually dissolved in the body, and, at the same time, they are replaced by new living tissue [31]. Since natural tissues can repair and renew themselves throughout life, bioresorbable materials are the optimal solution to produce high-performance bone implants [23]. In fact, in this way, the problems associated with the long-term stability of the implant are prevented, since the living tissue gradually replaces the prosthesis itself. Their mechanical performance gives the main issue related to resorbable biomaterials over the period required for the substitution when living tissues are still forming, and the implanted material is already being dissolved. The strength and stability of the interface should survive during the degradation process. Moreover, the resorption rate and the host tissue formation rate must match.

To adjust the dissolution rate, several methods can be used, such as the addition of doping elements to the biomaterial or the adjustment of the shape and size of the bioresorbable device [31]. Moreover, the substances released by the biomaterial during its dissolution must be acceptable to the human metabolism. On account of this criticism, a new target is to dope biodegradable materials with substances that may induce genetic stimulation [32,33]. In this

way, the natural healing of tissue can be favored. Some resorbable biomaterials are currently used in clinical practice. For example, polymers such as polylactic acid and polyglycolic acid are employed for the sutures [23]. These materials can withstand for an appropriate time, and then they are metabolized to CO_2 and H_2O . Even some ceramic materials, such as tricalcium phosphate, may be resorbable if they are used in porous devices or particulate form. However, these materials cannot undergo high mechanical stresses during the resorption phase [34].

1.6 Bioceramics

A bioceramic is defined as a ceramic used as a biomaterial; on the other hand, the broad term ceramic generally is defined as “an inorganic non-metallic material processed or consolidated at high temperatures.” The field of bioceramics is relatively new; it did not exist until the 1970s. However, many bioceramics are not new materials. One of the most important is Al_2O_3 , which we first encountered as a constituent of many traditional ceramic products. Bioceramics are typically classified into subgroups based upon their chemical reactivity in the body. Biomaterials in the United States: The subgroups are listed in Table 1.6-1, and Figure 1.6-1 shows the bioactivity spectrum of some bioceramics of clinical interest.

Table 1.6-1 Classification schema for bioceramics. Adapted from [35]

Nearly inert bioceramics
Examples: Al_2O_3 , low-temperature isotropic (LTI) carbon; ultra LTI carbon; vitreous carbon; ZrO_2
Tissue attachment: Mechanical
Bioactive ceramics
Examples: HA; bioactive glasses; bioactive glass-ceramics
Tissue attachment: Interfacial bonding
Resorbable bioceramics
Examples: Tricalcium phosphate (TCP); calcium sulfate; trisodium phosphate
Tissue attachment: Replacement
Composites
Examples: HA/autogenous bone; surface-active glass ceramics/poly(methyl methacrylate) (PMMA); surface-active glass/ metal fibers; polylactic acid (PLA)/carbon fibers; PLA/HA; PLA/calcium/phosphorus-based glass fibers
Tissue attachment: Depends on materials

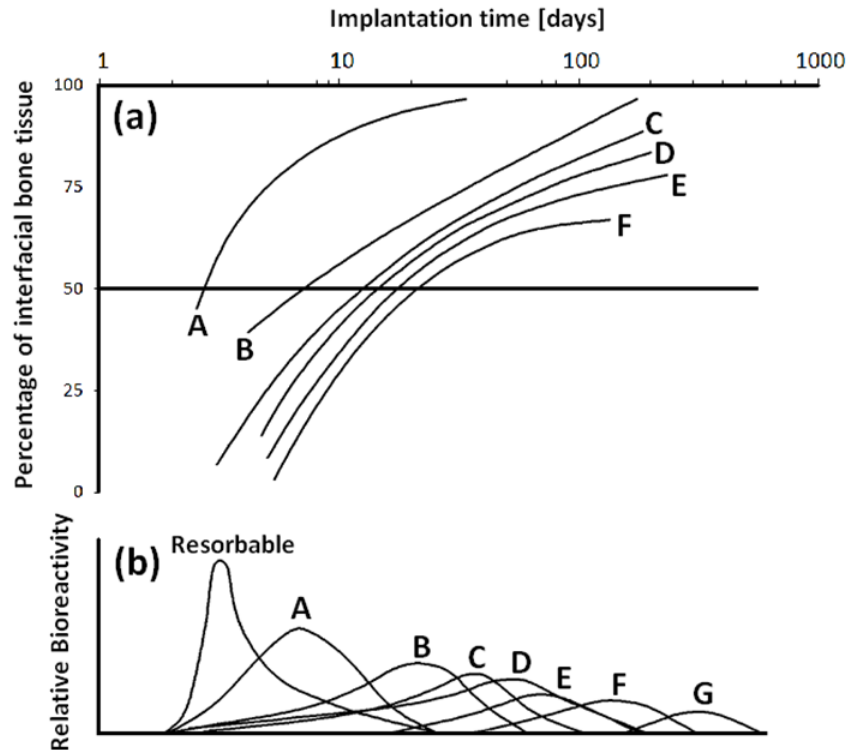


Figure 1.6-1 Bioactivity spectrum for various bioceramic implants:

(a) time dependence of the formation of bone-bonding at the implant interface, and (b) relative rate of bioreactivity

A: Bioglass® 45S5, B: KGS glass-ceramic, C: Bioglass® S53P4, D: A/W glass-ceramic,

E: dense synthetic HA, F: KGX glass-ceramic, G: Al₂O₃. Adapted from [36]

The first bioceramic employed in clinical applications was high-purity alumina. Such oxide has good biocompatibility, high chemical durability, and excellent tribological properties. Therefore, it is used in total hip prostheses and dental implants. Limitations in the use of alumina are due to its weak flexural strength. Moreover, alumina may induce stress shielding of bones. This effect is due to the difference between the stiffness of bone tissue and that of alumina, which are respectively about 7-25 GPa (for cortical bone) and 400 GPa. This means that the mechanical load is borne almost entirely by the alumina prosthesis. Thus, the bone stresses become subnormal (i.e., the remaining host bone is “shielded” by the implant). This alters the natural remodeling of the bone, and therefore the stress shielding can induce the cancellous bone to atrophy or even cause the loss of the implant. Accordingly, it is necessary to consider all aspects of the design of a prosthesis very carefully. Finally, another problem with alumina is

that it can be degraded in the body environment. However, alumina with adequate purity and microstructure is expected to have a lifespan of 30 years under load conditions. Since this is the life expectancy of a hip prosthesis, this ceramic can be successfully used for this application. Alumina non-cemented cups press-fitted into the acetabulum of the hip are quite frequent. An additional way to apply the bioinert ceramics, such as alumina and zirconia, is to employ them in a porous form, which promotes the ingrowth of bone tissues [36,37].

References

- [1] F. Barrère, C. A. van Blitterswijk and K. de Groot, "Bone regeneration: molecular and cellular interactions with calcium phosphate ceramics," *International Journal of Nanomedicine*, vol. 1, no. 3, pp. 317-332, 2006.
- [2] J. B. Kerr, Atlas of functional histology, London: Harcourt Publishers, 2000.
- [3] K. A. Hing, "Bone repair in the twenty-first century: biology, chemistry or engineering?," *Philosophical Transactions of the Royal Society of London. Series A: Mathematical, Physical and Engineering Sciences*, vol. 362, pp. 2821-2850, 2004.
- [4] "Surveillance, Epidemiology and End Results SEER. Structure of bone tissue.," 2006. [Online]. Available: http://training.seer.cancer.gov/module_anatomy/unit3_2_bone_tissue.html.
- [5] "University of Michigan. Bone structure.," 2006. [Online]. Available: <http://www.engin.umich.edu/class/bme456/bonestructure/bonestructure.htm>.
- [6] "smart service medical art," [Online]. Available: <https://smart.servier.com/>.
- [7] D. T. Reilly and A. H. Burstein, "Review article. The mechanical properties of cortical bone.," *J Bone Joint Surg Am*, vol. 56, pp. 1001-1022, 1974.
- [8] C. M. Ford and T. M. Keaveny, "The dependence of shear failure properties of trabecular bone on," *J Biomech*, vol. 29, pp. 1309-1317, 1996.
- [9] S. Ramakrishna, M. Ramalingam, T. S. Kumar and W. O. Soboyejo, "Basics of Human Biology," in *Biomaterials: a Nano Approach*, CRC Press, 2016, pp. 48-49.
- [10] A. R. Gideon, "Bone homeostasis," *Proc. Natl. Acad. Sci. USA*, vol. 95, p. 13361-13362, 1998.
- [11] S. C. Cowin, "Mechanical modeling of the stress adaptation process in bone," *Calcified Tissue International*, vol. 36, no. S1, 1984.
- [12] E. Seeman, "Bone quality: the material and structural basis of bone strength," *Journal of Bone and Mineral Metabolism*, vol. 26, no. 1, pp. 1-8, 2008.
- [13] G. Duque, "Bone and fat connection in aging bone," *Current Opinion in Rheumatology*, vol. 20, no. 4, pp. 429-434, 2008.

- [14] T. Gong, J. Xie, J. Liao, T. Zhang, S. Lin and Y. Lin, "Nanomaterials and bone regeneration," *Bone Research*, vol. 3, no. 1, 2015.
- [15] T. Nyary and B. E. Scammell, "Principles of bone and joint injuries and their healing," *Surgery (Oxford)*, vol. 33, no. 1, pp. 7-14, 2015.
- [16] W. T. Jia, C. Q. Zhang, J. G. Sheng and al, "Free vascularized fibular grafting in combination with a locking plate for the reconstruction of a large tibial defect secondary to osteomyelitis in a child: a case report and literature review," *J Pediatr Orthop*, vol. 19, pp. 66-70.
- [17] C. Laurencin, Y. Khan and S. F. El-Amin, "Bone graft substitutes," *Expert Rev Med Devices*, vol. 3, pp. 49-57, 2006.
- [18] J. C. Banwart, M. A. Asher and R. S. Hassanein, " Iliac crest bone graft harvest donor site morbidity.," *Spine (Phila Pa 1976)*, vol. 20, pp. 1055-1060, 1995.
- [19] C. Delloye, "Tissue allografts and health risks," *Acta Orthop Belg*, vol. 60, no. 1, pp. 62-67, 1994.
- [20] P. Ducheyne, *Comprehensive biomaterials*, Amsterdam: Elsevier, 2011.
- [21] M. Vallet-Regi, *Bio-Ceramics with Clinical Applications*, John Wiley & Sons, 2014.
- [22] D. Shi, *Biomaterials and tissue engineering*, Berlin: Springer, 2011.
- [23] B. D. Ratner, A. S. Hoffman, F. J. Schoen and J. E. Lemons, *Biomaterials Science: An Introduction to Materials in Medicine*, Elsevier Academic Press , 2004.
- [24] M. Vallet-Regi, "Evolution of bioceramics within the field of biomaterials," *Comptes*, vol. 13, pp. 174-185, 2009.
- [25] L. L. Hench, "Biomaterials: a forecast for the future," *Biomaterials*, vol. 19, pp. 1419-1423, 1998.
- [26] A. A. Hofmann, T. D. Goldberg, A. M. Tanner and T. M. Cook, "Surface cementation of stemmed tibial components in primary total knee arthroplasty," *The Journal of Arthroplasty*, vol. 21, pp. 353-357, 2006.
- [27] L. L. Hench, "The story of bioglass," *Journal of Materials Science: Materials in Medicine*, vol. 17, pp. 967-978, 2006.
- [28] L. L. Hench, R. J. Splinter, T. K. Geenlee and W. C. Allen, "Bonding mechanisms at the interface of ceramic prosthetic materials," *Journal of Biomedical Materials Research*, vol. 5, pp. 117-141, 1971.
- [29] T. Kokubo and H. Takadama, "How useful is SBF in predicting in vivo bone bioactivity?," *Biomaterials*, vol. 27, pp. 2907-2915, 2006.
- [30] M. Bohner and J. Lemaître, "Can bioactivity be tested in vitro with SBF solution?," *Biomaterials*, vol. 30, pp. 2175-2179, 2009.
- [31] M. Bohner, "Resorbable biomaterials as bone graft substitutes," *Materials Today*, vol. 13, pp. 24-30, 2010.

- [32] L. L. Hench and J. Wilson, An introduction to bioceramics, Singapore: World Scientific Publishing Co Pte Ltd, 1993.
- [33] L. L. Hench, "Genetic design of bioactive glass," *Journal of the European Ceramic Society*, vol. 29, pp. 1257-1265, 2009.
- [34] D. S. Metsger, T. D. Driskell and J. R. Paulsrud, "Tricalcium phosphate ceramic-a resorbable bone implant: review and current status," *The Journal of the American Dental Association*, vol. 105, p. 1035, 1982.
- [35] C. B. Carter and M. G. Norton, "Ceramics in Biology and Medicine," in *Ceramic Materials: Science and Engineering*, New York, NY, Springer, 2007, p. 636.
- [36] L. L. Hench, "Bioceramics," *Journal of the American Ceramic Society*, vol. 81, pp. 1028-1705, 1998.
- [37] K. S. Katti, "Biomaterials in total joint replacement," *Colloids and Surfaces B: Biointerfaces*, vol. 39, pp. 133-142, 2004.
- [38] "Commercial Opportunities from an Aging Population," *Business Insights*, 2004.

Chapter Two

Hydroxyapatite

Hydroxyapatite (HA) is a bioceramic widely studied due to its chemical similarity with the mineral component of bones. Besides, it is biocompatible, bioactive and thermodynamically stable in the body fluid, which poses it as an attractive material for a wide range of applications in the biomedical field. This chapter justifies the choice of hydroxyapatite as the material studied in this thesis and describes its main features along with the different methods of synthesis, and its applications in the medical field.

2.1 Calcium phosphate bioceramics

Calcium phosphate bioceramics have been in use in medicine and dentistry for more than 20 years. The interest in one group member, hydroxyapatite, arises from its similarity to bone apatite, the main component of the inorganic phase of bone, which plays a key role in the calcification and resorption processes of bone [1]. In the mid-1970s, three groups, Jarcho et al. in the USA, de Groot et al. in Europe, and Aoki et al. in Japan, simultaneously but independently worked toward the development and commercialization of hydroxyapatite as a biomaterial for bone repair, augmentation, and substitution. Different phases of calcium phosphate ceramics can be used in medicine, depending on whether a bioactive or a resorbable material is desired. Table 2.1-1 lists calcium phosphates that are often encountered in research and clinical in use.

Table 2.1-1 Family of calcium phosphate compounds. Adapted from [2]

Mineral Name	Chemical Name	Chemical Formula	Ca:P (Molar Ratio)
Monetite	Dicalcium phosphate (DCP)	CaHPO_4	1.00
Brushite	Dicalcium phosphate dihydrate (DCPD)	$\text{CaHPO}_4 \cdot 2\text{H}_2\text{O}$	1.00
	Octocalcium phosphate (OCP)	$\text{Ca}_8(\text{HPO}_4)_2(\text{PO}_4)_4 \cdot 5\text{H}_2\text{O}$	1.33
Whitlockite		$\text{Ca}_{10}(\text{HPO}_4)(\text{PO}_4)_6$	1.43
	Tricalcium phosphate (TCP)	$\text{Ca}_3(\text{PO}_4)_2$	1.50
Hydroxyapatite	Hydroxyapatite (HA)	$\text{Ca}_{10}(\text{PO}_4)_6(\text{OH})_2$	1.67
Hillinstockite	Tetracalcium phosphate (TTCP)	$\text{Ca}_4\text{P}_2\text{O}_9$	2.00

The stable phases of calcium phosphate ceramics depend considerably on the temperature and the presence of water, either during materials processing or in the in-service environment. At body temperature, only two calcium phosphates are stable when in contact with aqueous media such as body fluids. At $\text{pH} < 4.2$, the stable phase is $\text{CaHPO}_4 \cdot 2\text{H}_2\text{O}$ (brushite), while at $\text{pH} > 4.2$, the stable phase is $\text{Ca}_{10}(\text{PO}_4)_6(\text{OH})_2$ (hydroxyapatite). At higher temperatures, other phases such as $\text{Ca}_3(\text{PO}_4)_2$ (TCP) and $\text{Ca}_4\text{P}_2\text{O}_9$ (TTCP) are present. The unhydrated high-temperature calcium phosphate phases interact with water or body fluids at 37°C to form hydroxyapatite (HA) [2].

2.2 Biological apatites

Biological apatites constitute the mineral phase of calcified tissues such as bone, dentine, and enamel in the body and also some pathological calcifications. They are similar to synthetic HA, but they differ from HA in composition, stoichiometry, and physical and chemical properties. Biological apatites are usually calcium-deficient as a result of various substitutions at regular HA lattice points. It is, therefore, not appropriate to simply refer to biological apatite as hydroxyapatite.

2.2.1 Composition and structure

The general chemical formula for biological apatites is:



Where M represents metallic elements such as Na, K, and Mg; and Y represents functional groups such as acid phosphate, sulfates, etc. As compared to synthetic HA with the chemical formula of $\text{Ca}_{10}(\text{PO}_4)_6(\text{OH})_2$, substitution in biological apatites by carbonate group for the phosphate group takes place in a coupled manner, i.e. CO_3 for PO_4 and Na for Ca. The coupled substitution is necessary to balance charges for the replacement [2]. Differences in composition among apatites in human enamel and bone and HA are shown in Table 2.2-1.

Table 2.2-1 Composition of biological apatites and hydroxyapatite. Adapted from [2]

Major Constituent	Biological Apatite		Hydroxyapatite (wt%)
	In enamel (wt%)	In bone (wt%)	
Ca	36.00	24.50	39.60
P	17.70	11.50	18.50
Na	0.50	0.70	
K	0.08	0.03	
Mg	0.44	0.55	
F	0.01	0.02	
Cl	0.30	0.10	
CO₃²⁻	3.20	5.80	
Trace elements: Sr, Pb, Ba, Fe, Zn, Cu, etc.			
Ca:P (molar ration)	1.62	1.65	1.67

2.2.2 Properties

Because of substitutions and hence differences in composition, biological apatites possess different physical and mechanical properties, compared to synthetic HA. Table 2.2-2 lists the properties of apatites in human enamel and bone and HA.

Table 2.2-2 Properties of biological apatites and hydroxyapatite. Adapted from [2]

Property	Biological Apatite		Hydroxyapatite
	In enamel	In bone	
Lattice parameter /nm			
A	0.9441	0.9419	0.9422
C	0.6882	0.6880	0.6880
Crystal size /nm	130 × 30	25 × (2.5 – 5.0)	In micrometers
Elastic modulus /GPa	14	7 – 30	10
Tensile strength /MPa	70	50 – 150	~ 100

2.3 Hydroxyapatite

Hydroxyapatite belongs to the apatite family. Apatite is the name given to a group of crystals of the general chemical formula $M_{10}(RO_4)X_2$, where R is most commonly phosphorus, M could be one of several metals, although it is usually calcium, and X is commonly hydroxide or a halogen such as fluorine or chlorine. Possible M, R, and X are listed below [3]:

M = Ca, Sr, Ba, Cd, Pb, Mg, Na, K, etc

R = P, CO₃, V, As, S, Si, Ge, Cr, B, etc.

X = OH, CO₃, O, BO₂, F, Cl, Br, vacancy, etc.

The mineral, first called apatite in 1788 by Werner, had been confused earlier with other minerals such as aquamarine, olivine, and fluorite. Apatite minerals are found in almost all igneous rocks as well as in sedimentary and metamorphic rocks [4].

2.3.1 Structure

Hydroxyapatite is the most commonly used calcium phosphate in the medical field, as it possesses excellent biocompatibility and is osteoconductive. HA is bioactive, i.e., it supports bone ingrowth without breaking down and is stable in aqueous media with a pH range of 4.2 – 8.0, which lowers the risk of implant corrosion [4]. It has the chemical formula

$\text{Ca}_{10}(\text{PO}_4)_6(\text{OH})_2$ and a Ca/P molar ratio of 1.67. Its theoretical density is 3.156 g/cm^3 . The crystal structure of HA belongs to the hexagonal system, with the space group $\text{P6}_3/\text{m}$, and the unit cell parameters of $a = b = 0.942 \text{ nm}$, $c = 0.688 \text{ nm}$, $\alpha = \beta = 90^\circ$, $\gamma = 120^\circ$.

The crystal structure model of HAP is shown in Figure 2.3-1 [5]. As is shown, Ca^{2+} ions occupied two different positions in the unit cell. Four calcium atoms vertically distributed along the c -axis are called Ca(I), and the six calcium atoms arranged in a positive triangle around the c -axis are called Ca(II) [6,7]. Ca(I) is located at $c = 0$ and $c = 1/2$, which form a coordination polyhedron with the oxygen atoms in the surrounding nine PO_4^{3-} groups. Ca(II) occupies the positions of $c = 1/4$ and $c = 3/4$, and there are seven oxygen atoms around it, which are derived from six PO_4^{3-} groups and one OH^- group, respectively. PO_4^{3-} group has P as the central atom and four oxygen atoms coordinated to form a regular tetrahedral structure. OH^- is located at the center of an equilateral triangle formed by Ca and O perpendicular to the c -axis and at the four corners of the crystal structure [8].

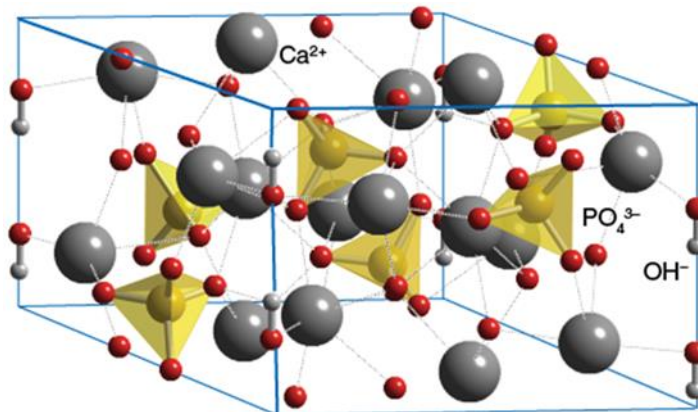
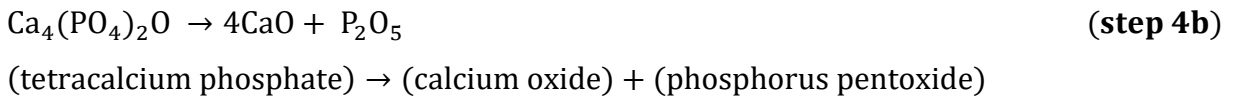
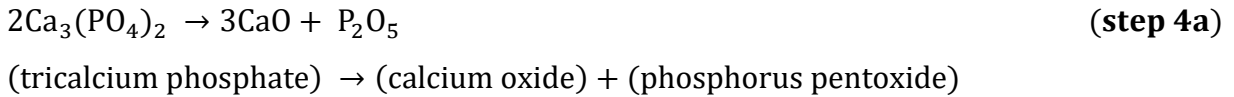
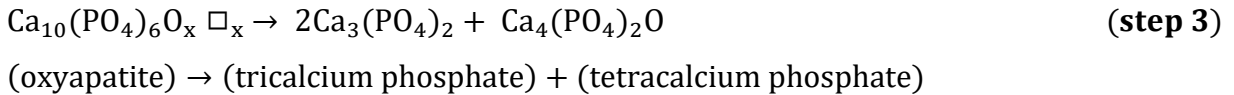
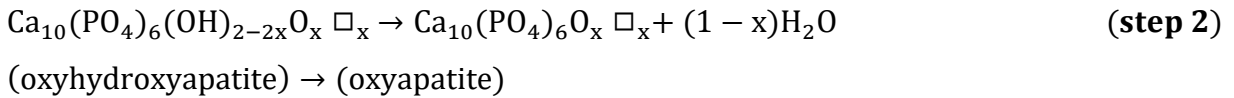
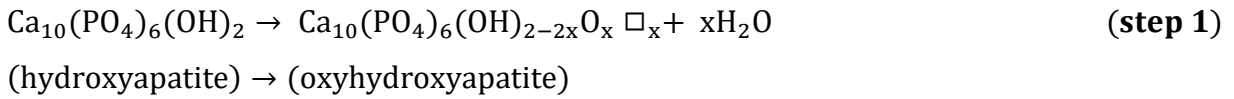


Figure 2.3-1 Crystal structure of hydroxyapatite. Adapted from [9]

Substituted apatites such as $\text{Ca}_{10}(\text{PO}_4)_6\text{F}_2$ and $\text{Ca}_{10}(\text{PO}_4)_6\text{Cl}_2$ have similar structures, with F and Cl substituting of OH in its position. The apatite structure is very hospitable in allowing the substitutions of many ions. Ca, PO_4 , and OH groups in apatite can be substituted. Carbonate (CO_3) can substitute either for the hydroxyl (OH) or the phosphate (PO_4) group, designated as type A or type B substitution, respectively. The substitutions cause morphological changes in precipitated apatite crystals as well as their properties. For example, CO_3 substituted apatite is more soluble than CO_3 -free synthetic apatite [22].

2.3.2 Thermal properties of HA

HA is usually processed by sintering, in order to obtain bulk components, or by plasma spraying, to produce coatings. Both methods imply heat treatments which are likely to degrade the original HA [10]. This is particularly true for the plasma spraying* process since the temperature of the plasma may exceed 15000 K [11]. Such a high temperature is known to degrade HA. The main processes which occur during the heat treatment of HA are dehydroxylation and decomposition [12]:



Where \square refers to lattice vacancies in the OH positions along the crystallographic c-axis in the structure of hydroxyapatite. Since HA powders are hygroscopic, a low-temperature thermal treatment removes the absorbed water by evaporation, but it does not cause any change in the HA structure. However, water is also present inside the HA lattice structure. Dehydroxylation occurs when HA loses $(\text{OH})^-$ groups at high temperatures. This process takes place in two steps with the formation of OHA and then OA (steps 1 and 2). If the temperature does not exceed a critical point, these new phases can be retransformed into HA in the presence of water [13]. Otherwise, if the critical temperature is surpassed, the HA crystal structure changes and suffers a complete and irreversible dehydroxylation. If the temperature increases further, HA starts to decompose. The decomposition of HA leads to the formation of other calcium phosphates (step

3) such as TCP and TTCP. These phases, in turn, can decompose into calcium oxide and phosphorus pentoxide (steps 4a and 4b). Approximate values for the dehydration and decomposition temperatures can be considered [14]:

< 800 °C	slow dehydroxylation
800 – 1350 °C	fast dehydroxylation
1350 °C	critical point: decomposition and irreversible dehydroxylation

However, the temperatures of HA modification are strongly influenced by various factors, such as heating rate, the initial state of the HA, and the environment. For example, a high degree of crystallinity of the starting HA usually reduces the tendency to decompose. Furthermore, the “real” composition of HA has remarkable importance. Raynaud et al. [15] observed that the degree of HA decomposition is strongly related to the Ca/P ratio. The Authors produced several HAs with a Ca/P ratio ranging from 1.5 up to 1.67. They treated such HAs at 1000°C for 15 hours. The Authors reported that a smaller value of the Ca/P ratio usually corresponded to a greater degree of decomposition. More than 90% of the HA with a Ca/P ratio of 1.51 decomposed to TCP after the heat treatment. On the contrary, the stoichiometric HA (Ca/P ratio of 1.67) showed much higher stability. The Authors also produced Ca-rich HAs, which, however, were found to be a biphasic mixture. The HA present in this composite was not degraded by heat treatment. Thus, the use of stoichiometric or Ca-rich HA is recommended to avoid decomposition.

The thermal stability of HA can also be increased using appropriate chemical substitutions. Chen and Miao [16] reported that replacing the OH⁻ group with F⁻ can increase the thermal stability of HA. When more than 60% of the OH groups are replaced, decomposition of the HA matrix is effectively restrained. Also, the environment in which the heating process takes place is very important to prevent the decomposition of HA, especially the partial pressure of water. Gross et al. reported that, with a partial water vapor pressure of 500 mm Hg, HA is stable up to about 20°C below its melting temperature. Instead, if the partial pressure of water is 900 mm Hg or higher, HA can be melted without decomposition. Therefore, processing HA in an atmosphere containing water vapor could reduce both dehydroxylation and decomposition [17].

2.3.3 Synthesis of HA

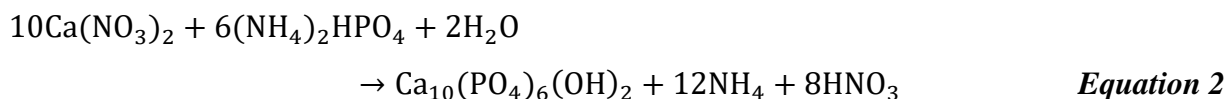
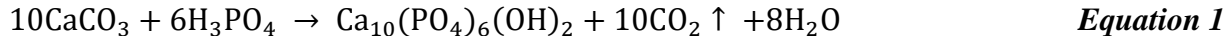
Many different routes can prepare synthetic hydroxyapatite powders. These can be generally split into three groups, aqueous reactions, solid-state reactions, and hydrothermal reactions.

i. Aqueous techniques

These may be split into two groups, precipitation, and sol-gel methods.

a) *Wet chemical precipitation*

Commercial preparations are generally produced by the precipitation method, which involves mixing reactants in the presence of water (usually at a controlled temperature, atmosphere, and pH) and leaving the resulting precipitate to age under conditions of continuous stirring for periods of up to 12 hours. Once aged, the precipitate is thoroughly washed. Filtered and dried. The two most common methods quoted in the literature are that of Rathje. (1939) (Equation 1), and Hayek and Newesely, (1963) (Equation 2).



In the first method (Equation 1), phosphoric acid is added dropwise to a stirred suspension of calcium carbonate in water. The process may be modified by the addition of ammonium hydroxide to keep the pH of the reaction alkaline to ensure that hydroxyapatite does not decompose after sintering [18]. In the second method (Equation 2), aqueous solutions of calcium nitrate and ammonium phosphate are prepared (again, ammonium hydroxide may be added to control the solution pH [19]). The phosphate solution is then added dropwise to the stirred calcium solution. This method is highly sensitive to the concentrations of the reactants and the solution pH for the formation of hydroxyapatite upon sintering.

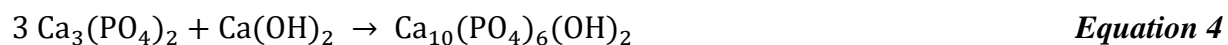
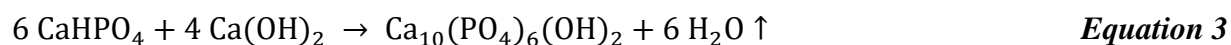
b) *Sol-gel*

The sol-gel method is a technique of homogeneous molecular mixing and low processing temperatures (<400°C) with the ability to synthesize nano-sized particles. This method includes

two stages: forming the ‘sol,’ which is a dispersion of solid particles, also known as colloids in a liquid, and the ‘gel,’ which can be defined as a biphasic system consisting of a solid and interstitial liquid phase. Gelation is the process of linking monomer units together through the condensation of OH^- forming $\text{M} - \text{O} - \text{M}$ bonds within the sol, causing the viscosity to increase. Gelation occurs by hydrolysis and polycondensation reactions. Precursor materials are mechanically mixed in a solvent at a pH that prevents precipitation. Typical precursors are metal alkoxides (e.g., tetraethoxysilane to introduce silicon) and metal salts (e.g., calcium nitrate to add calcium, and ammonium phosphate to add phosphorus) [20]. Some reactants are costly as compared to other low-temperature methods [21]. Post gelation, a drying process is necessary to remove the liquid phase. A significant amount of shrinkage usually accompanies drying. During drying, the gel can break into small pieces, resulting in a fine powder for further processing as a granulation.

ii. Solid-state reactions

In solid-state reactions, hydroxyapatite is produced via the stoichiometric mixing of reactants at specific temperatures. Examples of this method are given in equations 3 and 4. The calcium compounds are mixed, formed, and then sintered above 950°C [22].



iii. Hydrothermal Transformations

The third method of synthesizing hydroxyapatite is that of hydrothermal transformation. This process employs elevated temperatures, pressures and, controlled atmospheres to convert one substance into another via an exchange reaction. The reactions in equations 5 and 6 could be carried out hydrothermally by heating at 275°C under steam pressure of 84 MPa (12000psi). This route has the added benefit of preserving the original architecture, as in the production of porous hydroxyapatite from calcium carbonate corals or denatured bovine cancellous bone. Typical exchange reactions include that of Roy and Linnehan (1974) [23], which is carried out at $180\text{-}360^\circ\text{C}$ under 105 MPa for 12 - 48 hours (Equation 5), and Yamasaki et al. (1990) [24], which is carried out at 300°C under 30MPa for 2 hours (Equation 6).

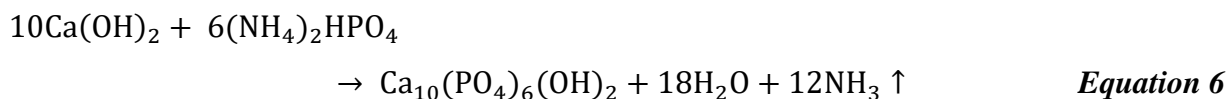
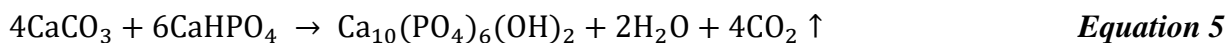


Table 2.3-1 Advantages and disadvantages of some of the synthesis methods for HA. Adapted from [25]

Method	Advantages	Disadvantages
Precipitation	<ul style="list-style-type: none"> – Simplicity – low operating costs – relatively inexpensive raw materials – low reaction temperatures – water is the only by-product. 	<ul style="list-style-type: none"> – difficulty in obtaining stoichiometric HA – need high pH to prevent the formation of Ca-deficient HA – need high sintering temperature to form crystalline HA – product sensitive to reaction conditions.
Hydrothermal	<ul style="list-style-type: none"> – HA can be produced in one step – energy efficient – environmentally friendly – high purity products can be synthesized – yields approaching 100%; – relatively low-cost reagents and short-time reaction. 	<ul style="list-style-type: none"> – batch sizes are limited to the size of the reaction vessel – high pressures required for processing.
Solid-state reaction	<ul style="list-style-type: none"> – Simple procedure – low cost – appropriate for mass-producing HA powder. 	<ul style="list-style-type: none"> – Needs high sintering temperature – long treatment times
Sol-gel process	<ul style="list-style-type: none"> – production of nano-HA particles – homogenous molecular mixing occurs – low processing temperature is required – increased control over phase purity. 	<ul style="list-style-type: none"> – difficulty to hydrolyze phosphate – expensive starting chemicals.

2.4 HA production method from biogenic resources

HA can be produced from naturally available waste resources. Apart from the conversion of low-cost wastes to a value-added product, HA produced from biogenic resources is suggested to have better biocompatibility due to its physicochemical similarity to natural bone apatite. The most common waste materials for HA productions include; bovine bones, fish bones, eggshells, and seashells. HA from biowastes has been an exciting field due to particular characteristics of the produced material and due to the economic and environmental benefits of waste reduction [26]. Eggshells are composed mainly of calcium carbonate, and therefore, it can be used as the calcium precursor source for HA. Generally, the shells are heated to 900 °C to remove organic compounds and to convert calcium carbonate to calcium oxide, which upon contact with the atmosphere is turned to calcium oxide. The obtained calcium hydroxide is then reacted with a proper phosphate source (such as di-ammonium hydrogen phosphate) to produce HA crystals. In some cases, the heating step has been replaced by chemical methods, such as direct treatment with HCl or HNO₃ to produce calcium nitrate or calcium chloride [5]. Regarding the phosphate sources, Boonyang et al. (2001) compared three different phosphate precursors (NH₄)₂HPO₄, Ca₃(PO₄)₂, and H₃PO₄ and only (NH₄)₂HPO₄ and Ca₃(PO₄)₂ were reported as suitable compounds for the production of monophasic HA [27]. Calcium carbonate originated from marine species usually exhibits inherent porosity and interconnectivity similar to that found in human bone [28].

2.5 Clinical application of HA

Hydroxyapatite has been investigated and used in a range of different forms for clinical applications. It has been utilized as a dense, sintered ceramic for middle ear implant applications, and alveolar ridge reconstruction and augmentation, in porous form for orbital implants, as granules for filling bony defects in dental and orthopedic surgery, such as for spinal fusion and impaction grafting, and as a coating on metal implants. There are now numerous reports of the successful use of hydroxyapatite-coated femoral prostheses and acetabular cups, and clinical results indicate that these implants are especially successful for younger patients. Another successful clinical application of hydroxyapatite has been in polymer composites. The original concept of a bioceramic filler in a polymer composite was introduced by Bonfield et al. (1981)

to produce an analog of the mineral-reinforced organic matrix in cortical bone. The material developed by Bonefield and co-workers contain up to 50% hydroxyapatite in a polyethylene matrix, has a stiffness similar to cortical bone, has high toughness, and has been found to exhibit bone-bonding in vivo. The material has been used as an orbit implant for orbital floor fractures and volume augmentation and is now used in middle ear implants, commercialized under the trade name HAPEX® [29].

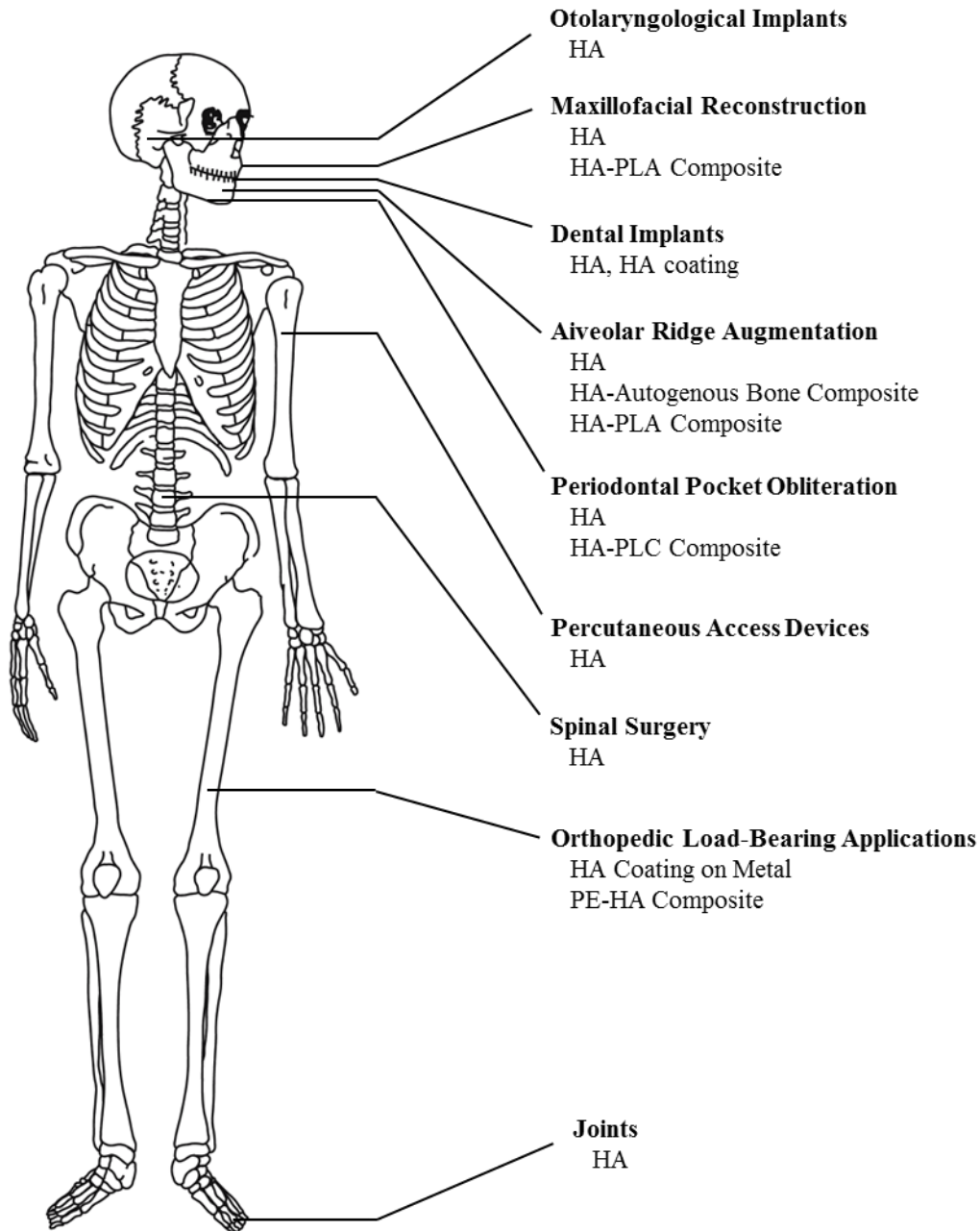


Figure 2.5-1 Illustration of the head-to-toe clinical uses of HA. Adapted from [30].

References

- [1] D. W. Fawcett, *A Textbook of Histology*, London: W. B. Company, 1986.
- [2] D. Shi, *Biomaterials and tissue engineering*, Berlin: Springer, 2011.
- [3] H. Aoki, *Medical Applications of Hydroxyapatite*, Tokyo, St. Louis: Ishiyaku EuroAmerica, 1994.
- [4] S. M. Best, A. E. Porter, E. S. Thian and J. Huang, "Bioceramics: Past, present and for the future," *Journal of the European Ceramic Society*, vol. 28, pp. 1319-1327, 2008.
- [5] M. Qi, K. He, Z. Huang and al, "Hydroxyapatite Fibers: A Review of Synthesis Methods," *JOM*, vol. 69, pp. 1354-1360, 2017.
- [6] J. D. Pasteris, B. Wopenka and E. Valsami-Jones, "Bone and Tooth Mineralization: Why Apatite?," *Elements*, vol. 4, no. 2, pp. 97-104, 2008.
- [7] B. Wopenka and J. D. Pasteris, "A mineralogical perspective on the apatite in bone," *Materials Science and Engineering: C*, vol. 25, no. 2, pp. 131-143, 2005.
- [8] M. I. Kay, R. A. Young and A. S. Posner, "Crystal Structure of Hydroxyapatite," *Nature*, vol. 204, pp. 1050-1052, 1964.
- [9] R. Reyes-García, P. Rozas-Moreno and M. Muñoz-Torres, "Cardiovascular disease and bone metabolism," *Endocrinología y nutrición*, vol. 58, no. 7, pp. 353-359, 2011.
- [10] F. H. Lin, L. Chun-Jen, C. Ko-Shao and S. Jui-Sheng, "Thermal reconstruction behavior of the quenched hydroxyapatite powder during reheating in air," *Materials Science and Engineering C*, vol. 13, pp. 97-104, 2000.
- [11] H. Herman, S. Sampath and R. McCune, "Thermal spray: current status and future trends," *MRS Bulletin*, vol. 25, pp. 17-25, 2000.
- [12] R. B. Heimann, "Thermal spraying of biomaterials," *Surface and Coatings Technology*, vol. 201, pp. 2012-2019, 2006.
- [13] "Effect of Ca/P Molar Ratio and Heat Treatment on Thermal Decomposition and Reconstitution of Hydroxyapatite," *Key Engineering Materials*, vol. 330–332, p. 107–110, 2007.

- [14] A. J. Ruys, M. Wei, C. C. Sorrell and al, "Sintering effects on the strength of hydroxyapatite," *Biomaterials*, vol. 16, pp. 409-415, 1995.
- [15] S. Raynaud, E. Champion, D. Bernache-Assollant and P. Thomas, "Calcium phosphate apatites with variable Ca/P atomic ratio I. Synthesis, characterisation and thermal stability of powders," *Biomaterials*, vol. 23, pp. 1065-1072, 2002.
- [16] Y. Chen and X. Miao, "Thermal and chemical stability of fluorohydroxyapatite ceramics with different fluorine contents," *Biomaterials*, vol. 26, pp. 1205-1210, 2005.
- [17] K. A. Gross and C. C. Berndt, "Thermal processing of hydroxyapatite for coating production," *Journal of Biomedical Materials Research*, vol. 15, pp. 580-587, 1998.
- [18] M. Akao, H. Aoki and K. Kato, "Mechanical Properties of Sintered Hydroxyapatite for Prosthetic Applications," *Journal of Materials Science*, vol. 16, pp. 809-812, 1981.
- [19] M. Jarcho, C. H. Bolen, M. B. Thomas, J. Bobick and al, "Hydroxylapatite Synthesis and Characterization in Dense Polycrystalline Form," *Journal of Materials Science*, vol. 11, pp. 2027-2035, 1976.
- [20] C. B. Carter and M. G. Norton, "Ceramics in Biology and Medicine," in *Ceramic Materials: Science and Engineering*, New York, NY, Springer, 2007, p. 636.
- [21] K. S. Katti, "Biomaterials in total joint replacement," *Colloids and Surfaces B: Biointerfaces*, vol. 39, pp. 133-142, 2004.
- [22] R. Z. Le Geros and J. P. Le Geros, "Dense Hydroxyapatite," in *An Introduction to Bioceramics*, Singapore, World Scientific, 1993.
- [23] D. M. Roy and S. K. Linnehan, "Hydroxyapatite Formed from Coral Skeletal Carbonate by Hydrothermal Exchange," *Nature*, vol. 247, pp. 220-222, 1974.
- [24] N. Yamasaki, T. Kai, M. Nishioka and al, "Porous Hydroxyapatite Ceramics Prepared by Hydrothermal Hot Pressing," *Journal of Materials Science*, vol. 9, pp. 1150-1151, 1990.
- [25] A. Fihri, C. Len, R. S. Varma and A. Solhy, "Hydroxyapatite: A review of syntheses, structure and applications in heterogeneous catalysis," *Coordination Chemistry Reviews*, vol. 347, pp. 48-76, 2017.
- [26] K. Gross and C. C. Berndt, "Biomedical Application of Apatites," *Reviews in Mineralogy and Geochemistry*, vol. 48, no. 1, pp. 631-672, 2002.
- [27] N. Neelakandeswari, G. Sangami and N. Dharmaraj, "Preparation and Characterization of Nanostructured Hydroxyapatite Using a Biomaterial," *Synth React Inorg M*, vol. 41, pp. 513-516, 2011.
- [28] K. A. Hing, "Bone repair in the twenty-first century: biology, chemistry or engineering?," *Philosophical Transactions of the Royal Society of London. Series A: Mathematical, Physical and Engineering Sciences*, vol. 362, pp. 2821-2850, 2004.

- [29] B. D. Ratner, A. S. Hoffman, F. J. Schoen and J. E. Lemons, *Biomaterials Science: An Introduction to Materials in Medicine*, Elsevier Academic Press , 2004.
- [30] L. L. Hench and J. Wilson, *An introduction to bioceramics*, Singapore: World Scientific Publishing Co Pte Ltd, 1993.

Part Two

Experimental Study

Chapter Three

Materials & Methods

This chapter outlines the experimental procedures followed to prepare hydroxyapatite along with a brief description of the characterization methods used. The hydroxyapatite powders were characterized by x-ray diffraction (XRD), Fourier transform infrared (FTIR) spectroscopy, and scanning electron microscope (SEM) in conjunction with energy dispersive x-ray spectroscopy (EDX) to provide information about crystal structure, composition, functional group distribution, and morphology.

3.1 Synthesis of Hydroxyapatite

3.1.1 Materials

Hydroxyapatite powders were prepared through wet chemical precipitation method using calcium hydroxide $\text{Ca}(\text{OH})_2$ (97%, Riedel-de Haën, Germany), and di-ammonium hydrogen phosphate $(\text{NH}_4)_2\text{HPO}_4$ (98%, Panreac, Spain). While distilled water and ethanol (96%, Biochem Chemopharma, Montreal) were used as solvents.

3.1.2 Experimental procedure

For preparing hydroxyapatite bioceramic, calcium hydroxide $\text{Ca}(\text{OH})_2$, and di-ammonium hydrogen phosphate $(\text{NH}_4)_2\text{HPO}_4$, were weighed using a digital analytical balance in amounts corresponding to the Ca/P ratio of 1.67.

The weighed powders were dispersed in a water-ethanol mixture with the ratio 1:1 for the calcium hydroxide and 1:2 for the di-ammonium hydrogen phosphate in two separate beakers. The precipitation was performed by slow addition of PO_4^{3-} solution to the Ca^{2+} solution under continuous stirring for 1h. After the complete addition, the produced HA suspension was allowed to mature for 24 hours while still being stirred.

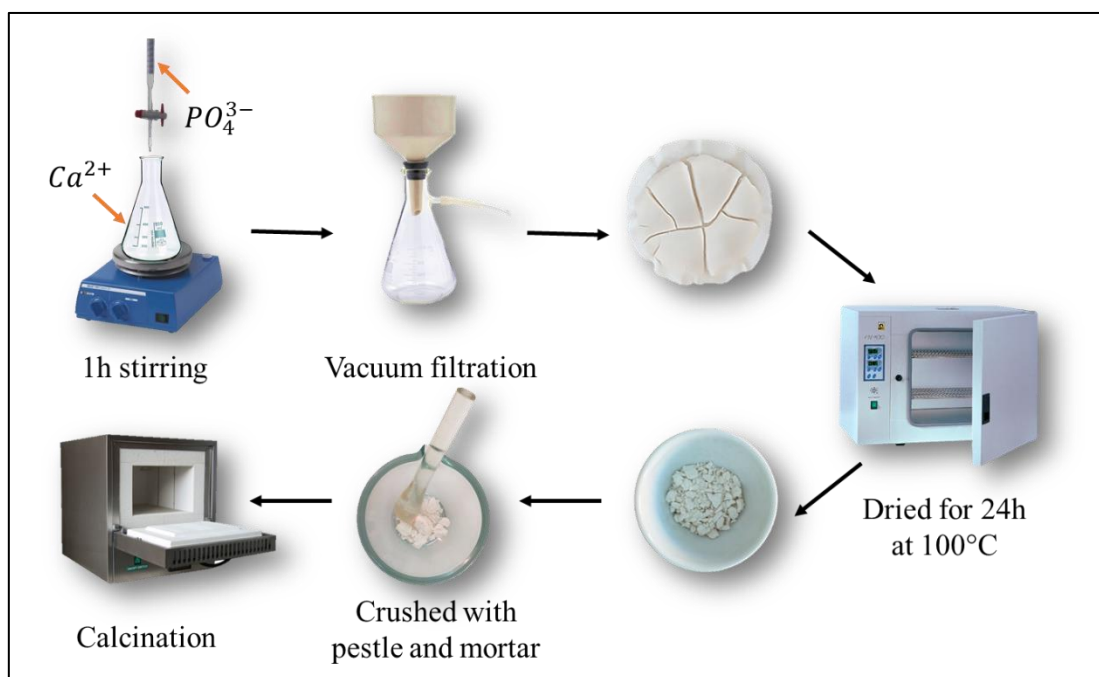


Figure 3.1-1 Schematic representation of the preparation steps of HA

As a result of this reaction, a milky white solution was obtained. During the whole process, the temperature was kept constant at room temperature (Figure 3.1-1). To remove any impurities, the precipitate was separated from the suspension by vacuum filtration, washed with distilled water, ethanol then acetone. The precipitate was oven-dried at 100°C for 24 hours and then ground to a powder using a porcelain pestle and mortar. In the next step, hydroxyapatite powder was heat-treated at 200°C, 500°C, 600°C, and 800°C for 4 hours at a rate of 5°C/min. The flow chart below in Figure 3.1-2 summarizes the steps of the synthesis of hydroxyapatite

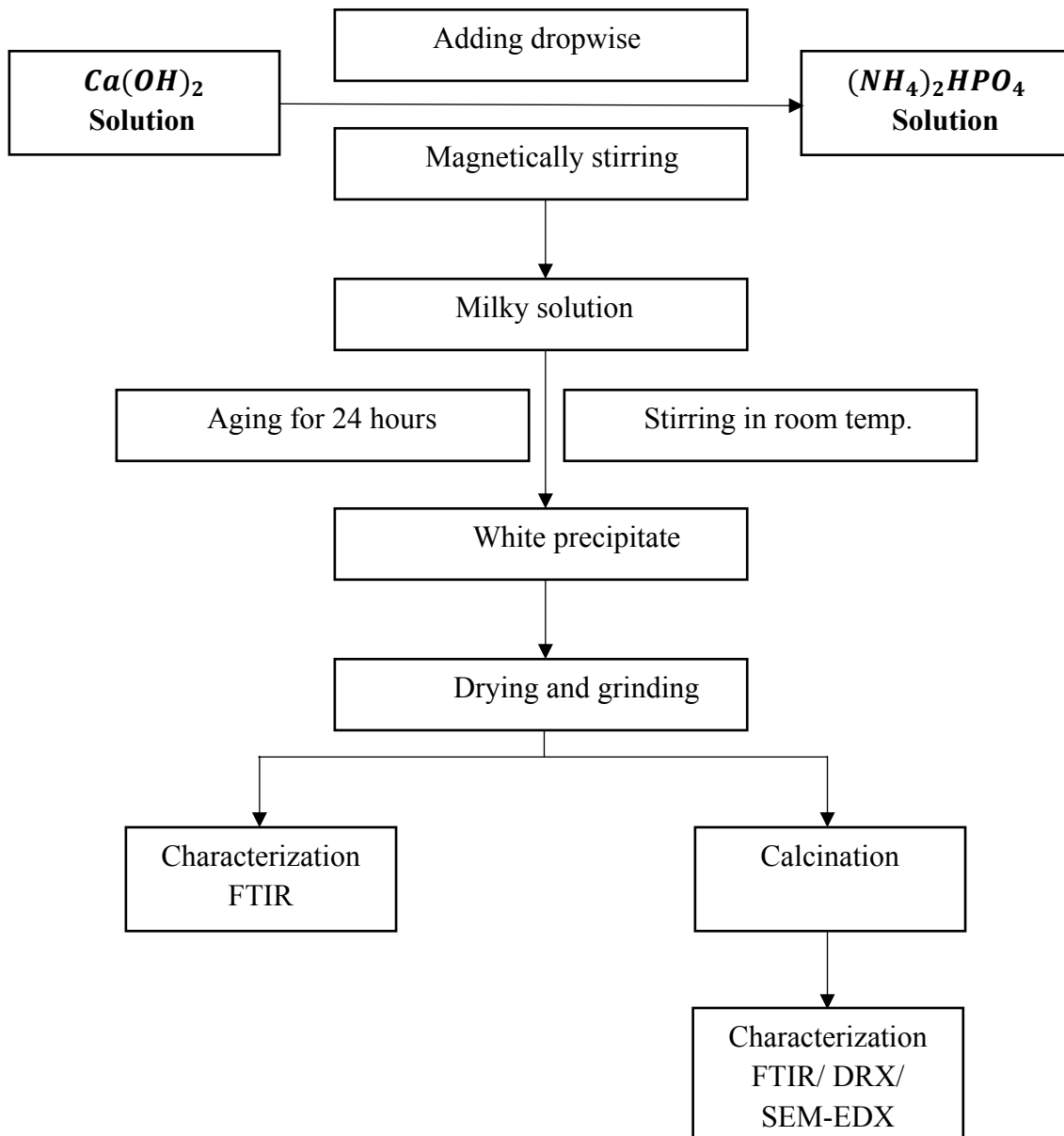


Figure 3.1-2 Flow chart of the synthesis of Hydroxyapatite

3.2 Characterization methods

3.2.1 X-Ray Diffraction

Max von Laue, in 1912, discovered that crystalline substances act as three-dimensional diffraction gratings for X-ray wavelengths similar to the spacing of planes in a crystal lattice. X-ray diffraction is now a common technique for the study of crystal structures and atomic spacing. X-ray diffraction is based on constructive interference of monochromatic X-rays and a crystalline sample. These X-rays are generated by a cathode ray tube, filtered to produce monochromatic radiation, collimated to concentrate, and directed toward the sample. The interaction of the incident rays with the sample produces constructive interference (and a diffracted ray) when conditions satisfy Bragg's Law:

$$n\lambda = 2d \sin \theta$$

Where n is a positive integer, λ is the wavelength of the X-rays, d is the distance between the different plane of atoms in the crystal lattice and θ is the angle of diffraction.

This law relates the wavelength of electromagnetic radiation to the diffraction angle and the lattice spacing in a crystalline sample. These diffracted X-rays are then detected, processed and counted. By scanning the sample through a range of 2θ angles, all possible diffraction directions of the lattice should be attained due to the random orientation of the powdered material. Conversion of the diffraction peaks to d-spacings allows identification of the mineral because each mineral has a set of unique d-spacings. Typically, this is achieved by comparison of d-spacings with standard reference patterns [4,5].

The prepared HA samples were analyzed by XRD using Siemens D5000 Diffractometer, with $\text{CuK}\alpha$ monochromated be. The scanning range 2θ was performed from 20° to 70° using a step size between 0.01 and 0.04° , and counting time from 2 to 10s.

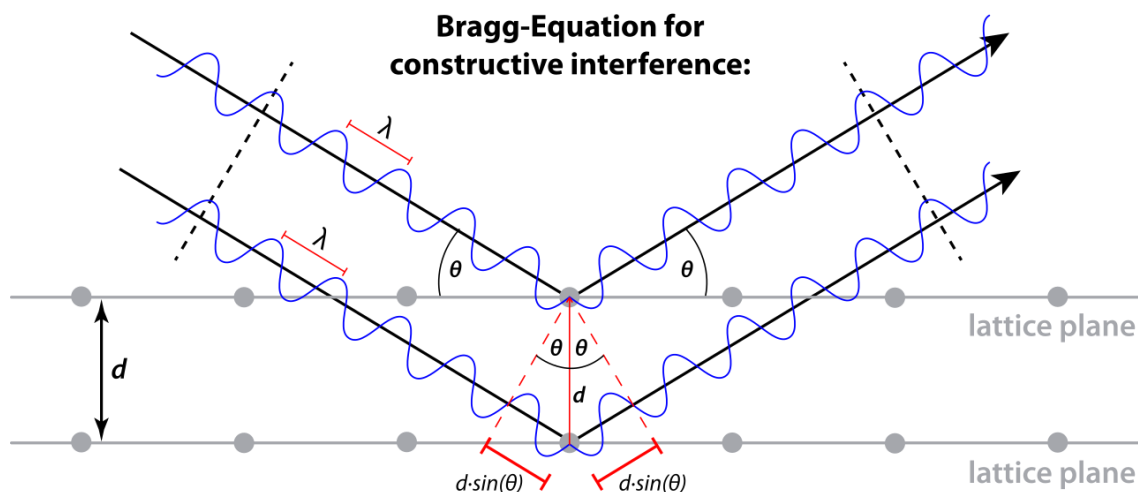


Figure 3.2-1 Illustration of Bragg's Law for constructive interference. Adapted from [1]

3.2.2 Fourier Transform Infrared Spectroscopy

Fourier transform infrared spectroscopy (FT-IR) is a chemical analysis technique that generates a molecular fingerprint of the samples. It is based on the vibrations of the atoms, which are subjected to passing infrared radiation and measures the ratio of the incident radiation that is absorbed at a particular energy. As the sample is exposed to different wavelengths of infrared light, transitions between vibrational energy levels of various chemical bonds are detected, allowing for the functional groups within the sample's molecules to be identified [3]. The resulting spectra, which are a characteristic of infrared absorption/emission at different wavelength, can be used to define the chemical composition of the sample.

In this study, FT-IR was used for further confirmation of the chemical composition of the samples. FT-IR spectroscopy was carried out by a Shimadzu FTIR-8400S. Sample preparation consisted of mixing 0.001g of hydroxyapatite powder with 0.2g of potassium bromide (KBr), compressed to form a tablet and then placed on the specimen holder to be analyzed at a range of 400 to 4000 cm^{-1} at 4 cm^{-1} resolution.



Figure 3.2-2 Shimadzu FTIR: 8400S

3.2.3 Scanning Electron Microscopy (SEM) & Energy Dispersive Analysis of X-ray (EDX)

Scanning electron microscopy (SEM) is a method for high-resolution imaging of surfaces. The SEM generates a beam of incident electrons in an electron column above the sample chamber. The electrons are produced by a thermal emission source, such as a heated tungsten filament, or by a field emission cathode. To create an SEM image, the incident electron beam follows a vertical path through the column. It passes the electromagnetic lens, which directs and focuses the beam on to the sample. Once the beam of electrons hits the sample, secondary electrons are ejected. Detectors will then collect the signals of the emitted secondary electrons, analyze and convert them to a three-dimensional image [2].

The beam of electrons emitted on the sample also produces x-rays. The energy dispersive x-ray (EDX) instrument collects the x-rays and converts them into useful information. Each element has a set of characteristic x-ray lines. The energy dispersive x-ray technique is utilized to identify the element and measure the composition of the sample material. The output from the EDX analysis is a spectrum, which is a plot of how frequently an x-ray is received for each energy level. An EDX spectrum normally displays peaks corresponding to the energy levels. These peaks are generally unique to an element. Higher peaks in the spectrum indicate higher concentrations in that element. Overlapping peaks from mixtures are deconvolved using specialized computer software. Energy dispersive x-ray systems are often attachments to scanning electron microscopy instruments. Typically scanning electron microscopy provides the visual analysis and energy dispersive x-ray provides the elemental analysis [6].

For this characterization, HA samples were prepared in discs. For doing so, 4.5 g of the material powder was pressed using a Specac hydraulic press with a load pressure of 2.5 tons.



Figure 3.2-3 Scanning Electron Microscope JEOL JSM-6390LV

References

- [1] "ETH Zürich," [Online]. Available: <https://www.microscopy.ethz.ch/bragg.htm>.
- [2] N. Erdman , D. C. Bell and R. Reichelt , "Scanning Electron Microscopy," in *Handbook of Microscopy*, Springer , 2019.
- [3] J. Ferraro and K. Krishnan, Practical Fourier transform infrared spectroscopy : Industrial and laboratory chemical analysis, San Diego: Elsevier, 2012.
- [4] C. Suryanarayana and M. G. Norton, X-Ray Diffraction: A Practical Approach, Springer , 1998.
- [5] B. D. Cullity and S. R. Stock, Elements of X-ray diffraction, Miejsce nieznane: Pearson India Education Services, 2015.
- [6] Y. V. Pathak , Handbook of metallonutraceuticals, CRC Press, 2016.

Chapter Four

Results & Discussion

This chapter presents the results and interpretation of the previous investigations concerning the crystal structure, composition, and morphology of the prepared hydroxyapatite

4.1 X-ray Diffraction analysis

The XRD patterns of hydroxyapatite powders heat-treated at 200, 500, and 600°C are shown in figures 4.1-1, 4.1-2, and 4.1-3, respectively. Based on the identification of the peaks in these patterns, we found the coexistence of two forms:

- a) Apatite of chemical formula : $H_2Ca_{10}O_{26}P_6$, according to the code **(98-026-1063)**, representing synthetic hydroxyapatite which structure is hexagonal with the following lattice parameters: ($a=b=9,4190 \text{ \AA}$, $c = 6,8810 \text{ \AA}$), and space group $P6_3/m$.
- b) Apatite-(CaOH) with the chemical formula: $H_{4.6}Ca_{9.63}O_{26.54}P_{5.78}$, according to the code **(98-015-0687)**, with hexagonal crystal structure, space group $P6_3/m$, and the following lattice parameters: ($a=b = 9,4700 \text{ \AA}$, $c = 6,8840 \text{ \AA}$).

➤ The quantification of the two structural forms is as follows:

Apatite represents the majority of the synthetic HA at different calcination temperatures of 200, 500 and 600°C and the rate increases with the increase of the thermal processing temperature.

The obtained results are summarized in the following table (see appendix):

Synthetic HA calcined at 200°C	Synthetic HA calcined at 500°C	Synthetic HA calcined at 600°C
Apatite : 69 % Apatite –CaOH : 31%	Apatite : 90 % Apatite –CaOH : 10%	Apatite : 90 % Apatite –CaOH : 10%

The XRD pattern of natural hydroxyapatite powder extracted from bovine bone is presented in the figure 4.1-4. This pattern shows, like the previous ones, the existence of two forms, the apatite phase and the apatite-CaOH phase. But in this case, it's the apatite-CaOH that represents the dominant phase, with a higher percentage (83%) than the apatite phase (17%). This indicates that a new element has been formed after the partial degradation of hydroxyapatite at a high temperature (800°C) (see appendix).

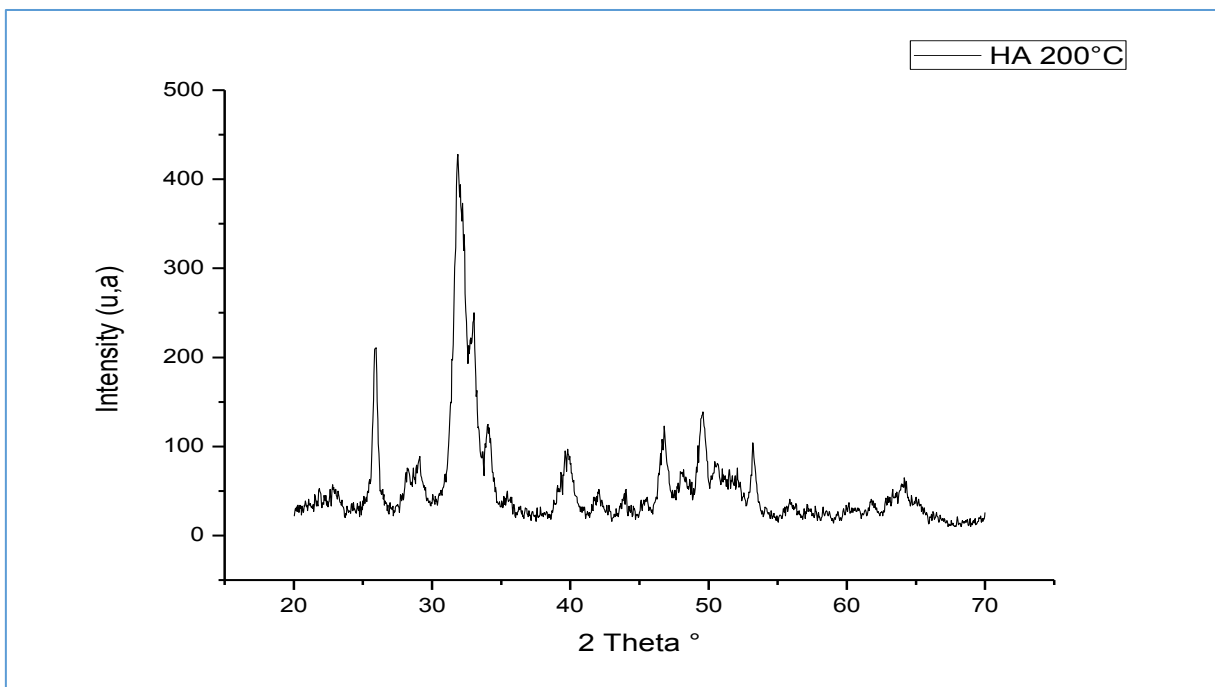


Figure 4.1-1 XRD pattern of HA heat-treated at 200°C

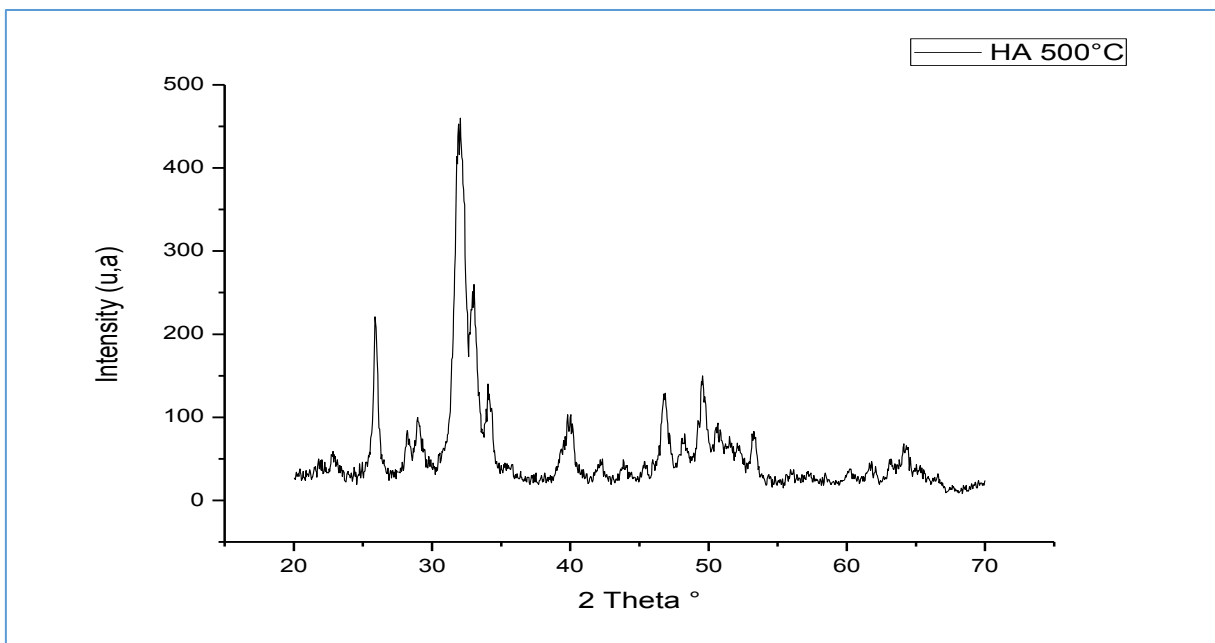


Figure 4.1-2 XRD pattern of HA heat-treated at 500°C

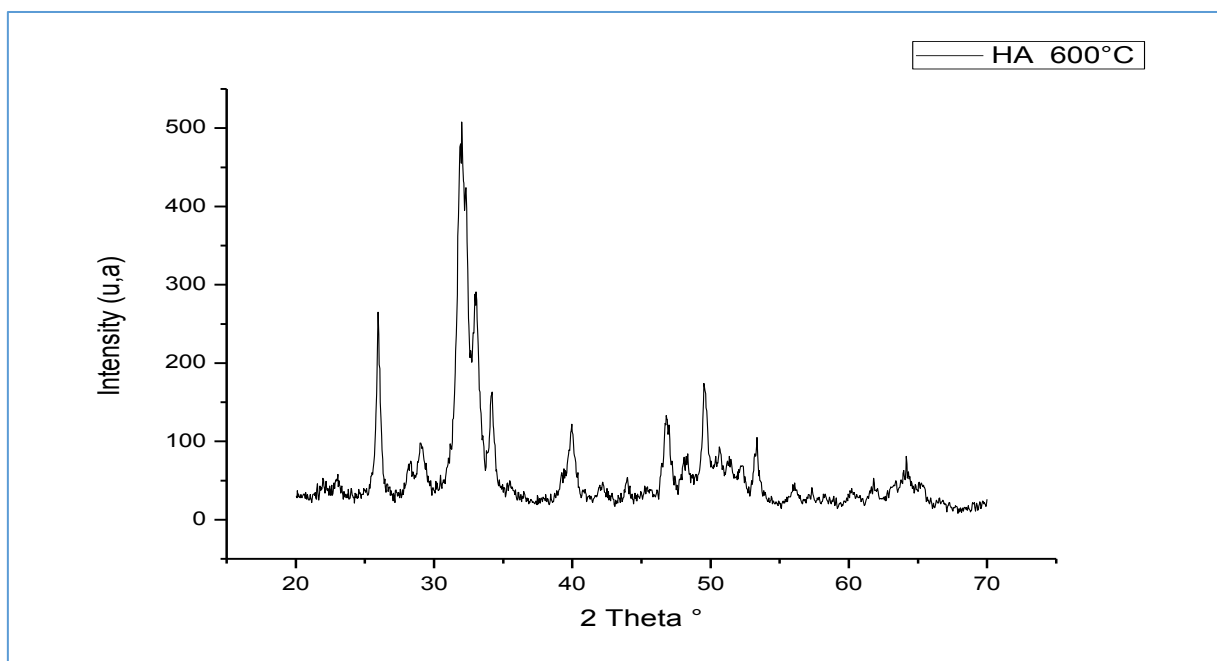


Figure 4.1-3 XRD pattern of HA heat-treated at 600°C

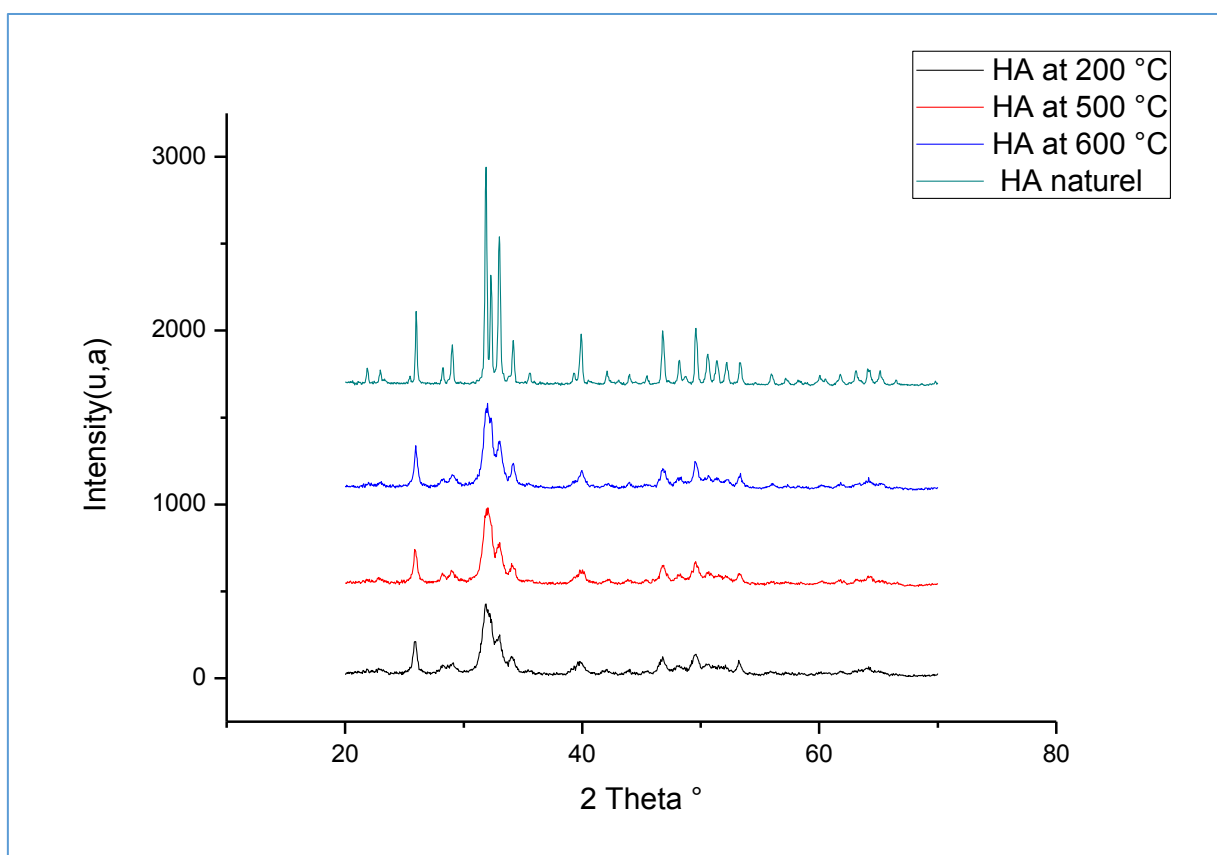


Figure 4.1-4 XRD patterns of synthetic and natural HA

4.2 Fourier Transform Infrared Spectroscopy (FTIR)

Figure 4.2-1 represents the FT-IR spectrum of hydroxyapatite powder at 100°C, it confirms the formation of hydroxyapatite containing the P – O and O – H bands of the phosphate and hydroxyl groups constituting hydroxyapatite. We observe a band at 1073 cm⁻¹ corresponding to the asymmetric stretching mode ν_3 of the PO₄³⁻ ions and a band at 565 cm⁻¹ corresponding to the bending mode (ν_4) of the PO₄³⁻ group. In addition, we observe a wide band between 3011–3688 cm⁻¹ and another one with low-intensity at 1653 cm⁻¹ corresponding is assigned to the bending mode of the H₂O molecules. The band at 876 cm⁻¹ is attributed to vibration mode of ν_4 (CO₃²⁻). In addition, the characteristic absorption band of the vibration frequencies of OH⁻ ions of the apatite network is located at 602 cm⁻¹. Comparison between the IR spectra of hydroxyapatite at 100 and 200°C (Figure 4.2-1 and 4.2-2) shows the evolution of hydroxyapatite according to temperature. The two IR spectra are mainly characterized by bands associated with an apatitic structure. We find that despite the change in temperature, IR spectra detect the same absorption bands with a slight deformation and an increase in intensity.

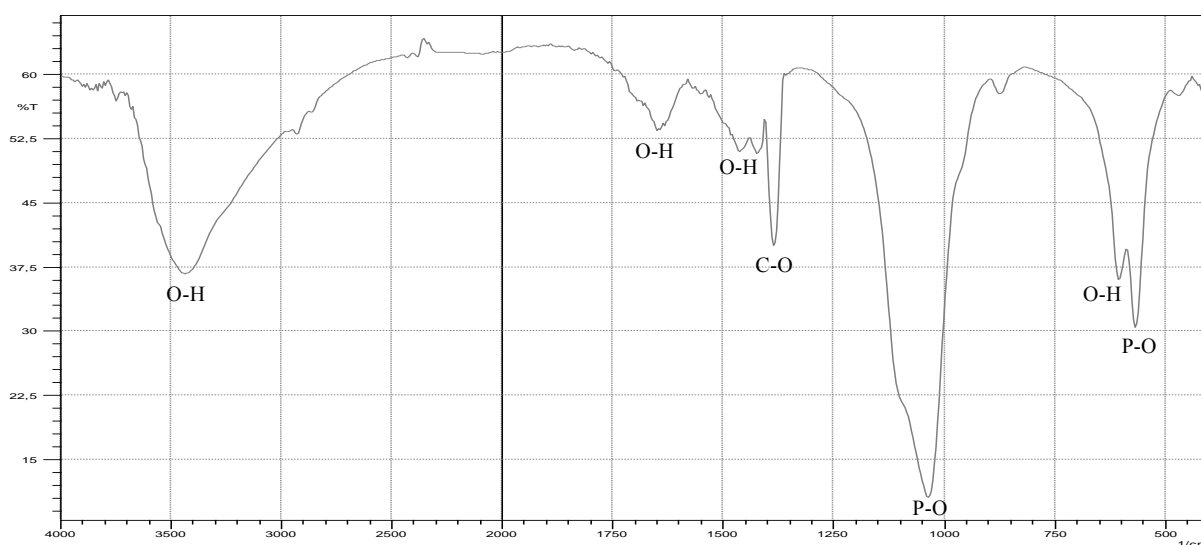


Figure 4.2-1 FTIR spectrum of HA at 100°C

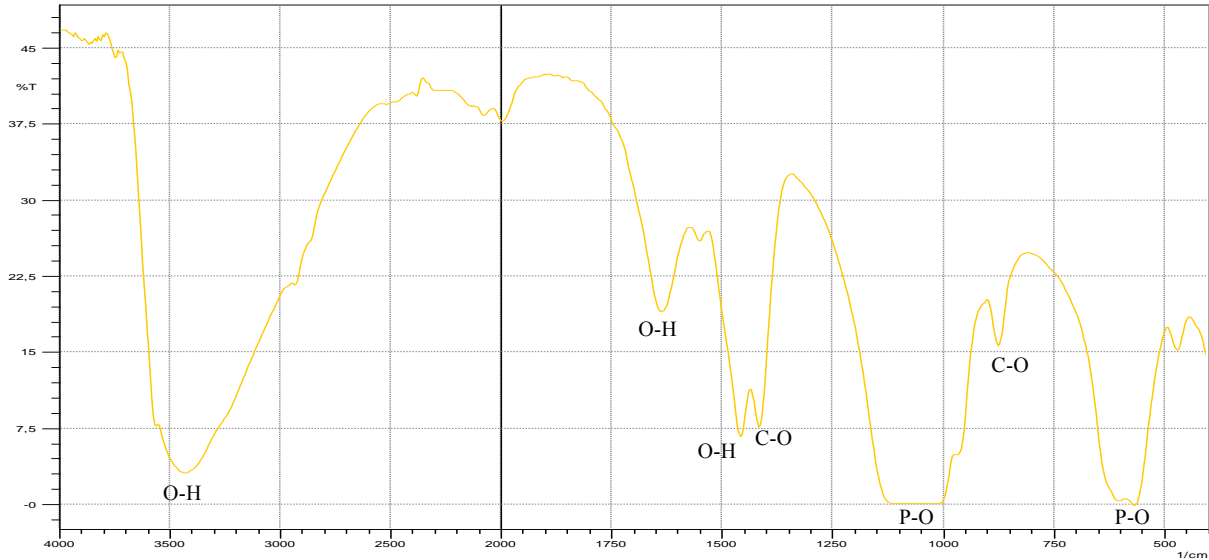


Figure 4.2-2 FTIR spectrum of HA at 200°C

4.3 Energy Dispersive X-Ray Analysis

According to the energy-dispersive X-ray spectroscopy spectra, the predominant elements in both samples are P and Ca without any sign of impurities. The intensity of the calcium peak is always higher than that of the phosphorus, since the concentration of Ca introduced during the synthesis process is higher than the phosphorus concentration (Figure 4.3-1 and 4.3-2). We also note two peaks corresponding to the Ca element, which confirms the results obtained by XRD (the existence of two structural forms (HA and HA-CaOH)).

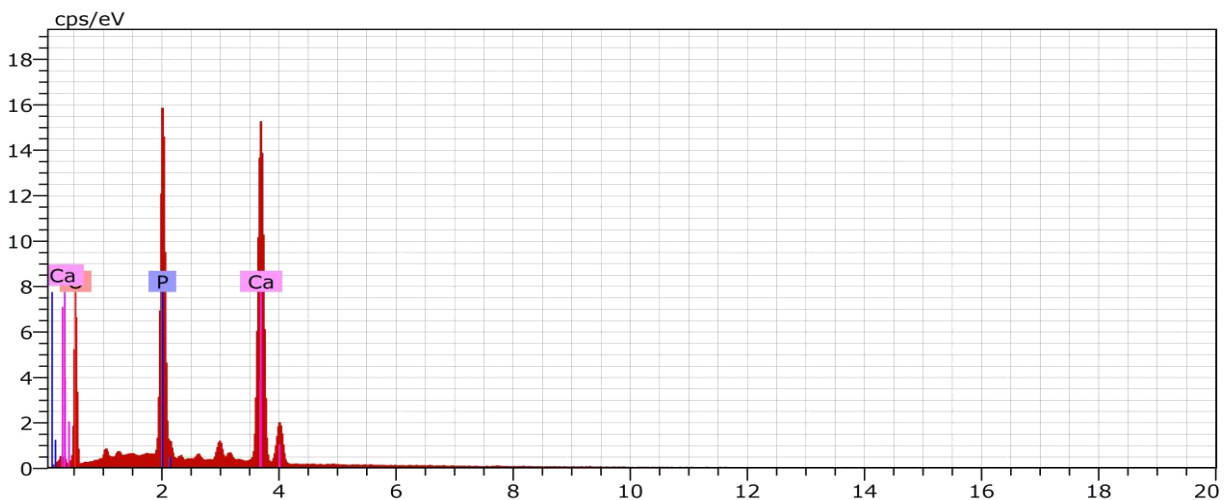


Figure 4.3-1 EDX pattern of synthetic HA calcined at 800°C

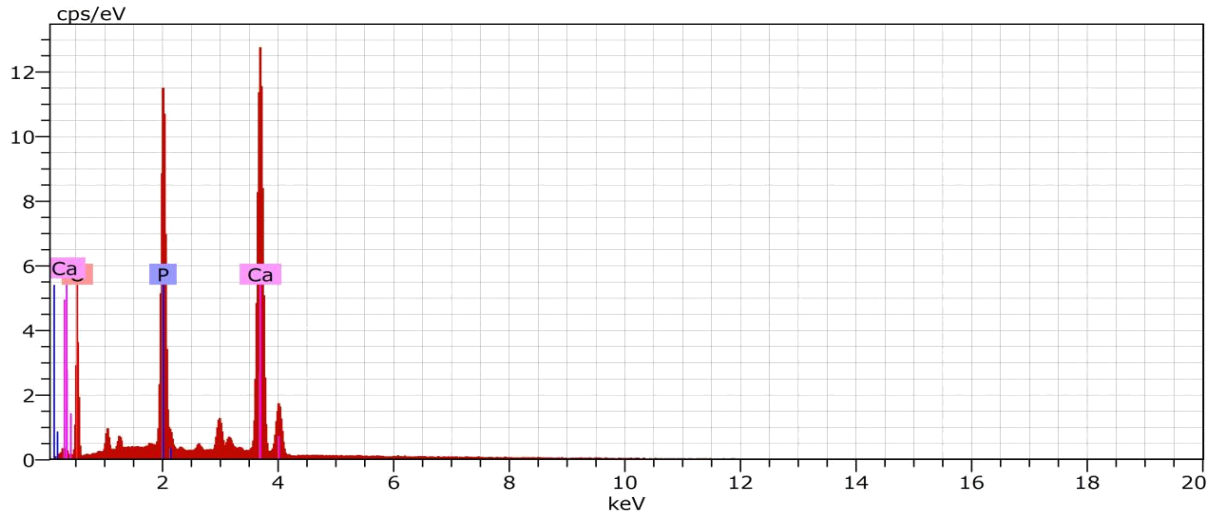


Figure 4.3-2 EDX pattern of natural HA extracted from bovine bone calcined at 800°C

4.4 Scanning Electron Microscopy

Figure 4.4-1 shows the SEM micrograph of the synthesized hydroxyapatite powder heat-treated at 200°C, we can see the appearance of irregular dense powder particles with vacancies between them. The SEM of synthetic HA heat-treated at 800°C (Figure 4.4-2) revealed a poorly crystallized and dense model, with an irregular, oval and spherical shape resembling lozenges. The micrograph of natural HA powder extracted from bovine bone calcinated at 800°C (Figure 4.4-3) presents a morphology of porous particles with smoother surfaces and a regular spherical shape.

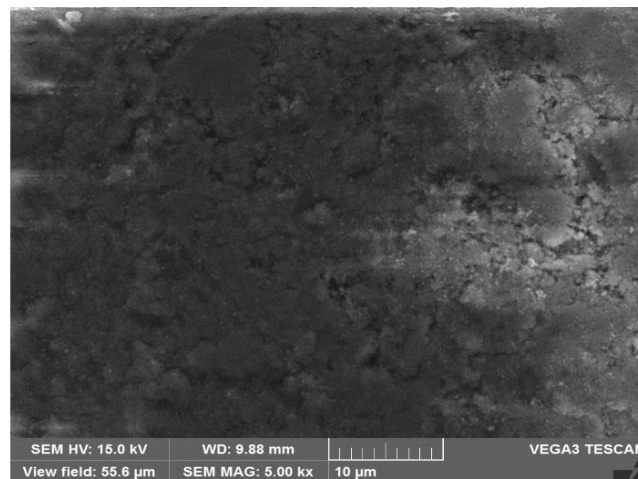


Figure 4.4-1 SEM image of synthetic HA at 200°C

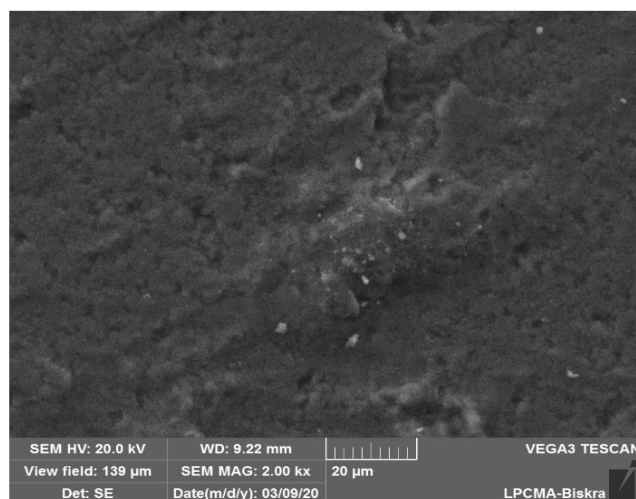


Figure 4.4-2 SEM image of synthetic HA at 800°C

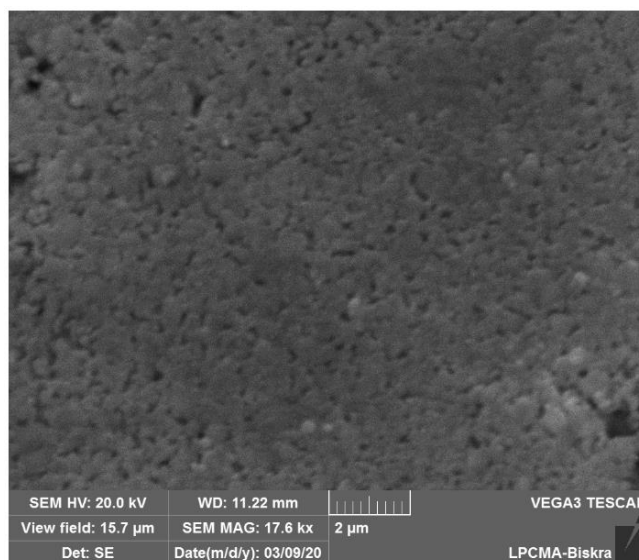


Figure 4.4-3 SEM image of natural HA extracted from bovine bone at 800°C

Conclusion & future work

Hydroxyapatite is a significant component of the human body, comprising 60% of bone, 97% of tooth enamel and 70% of dentin. HA is the most attractive member of the calcium phosphates family, and like the other ones is known as a bioceramic with specific advantages raise from chemical similarity to the mammalian inorganic structure. Its characteristics, including biocompatibility, bioactivity, osteoconduction and osteoinduction*, allow it to be used in a wide range of medical and dental applications.

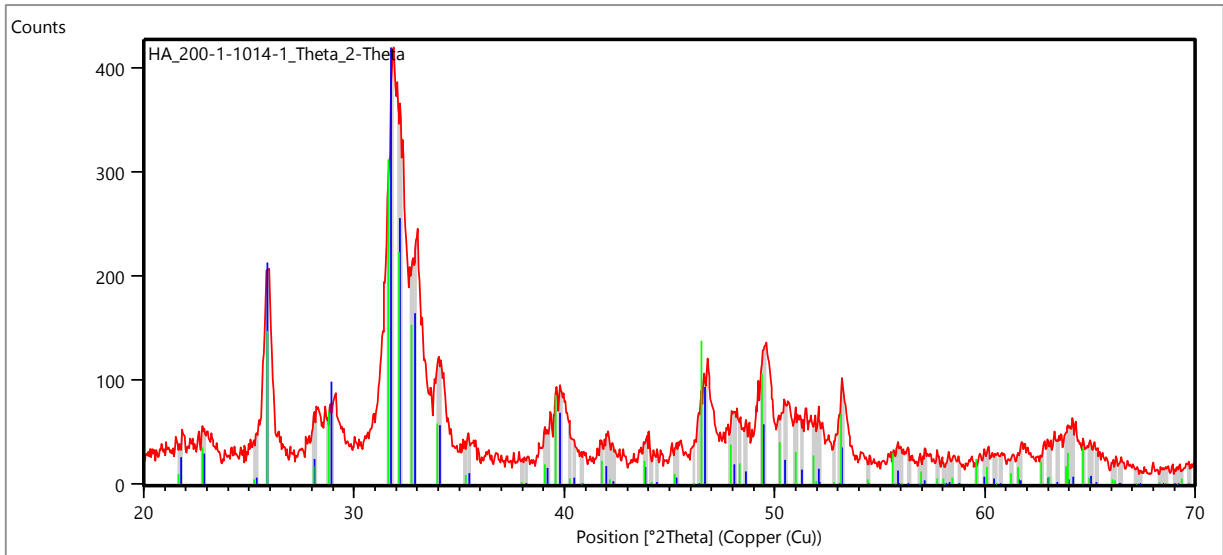
In this work, HA was synthesized using a simple laboratory approach, to demonstrate the influence of thermal treatment on the structure of hydroxyapatite powders. The reagents used for HA synthesis were diammonium hydrogen phosphate ($(\text{NH}_4)_2\text{HPO}_4$) and calcium hydroxide ($\text{Ca}(\text{OH})_2$) as P and Ca sources respectively. The prepared samples were evacuated at various temperatures up to 800°C, and the influence of the heat-treatment on the structure of this material was investigated using XRD, FTIR, and SEM-EDX.

- The XRD patterns of synthetic hydroxyapatite heat-treated at 200°C, 500°C, and 600°C, showed the apatitic structure (HA) of the analyzed powders with apatite as the dominant phase. While the XRD analysis of the natural hydroxyapatite (calcined at 800°C) revealed the peaks of (HA-CaOH) as the major phase. This study also shows that the crystallinity of HA powders increased as calcination temperature increased.
- From the FTIR spectrum, it was observed that the persistence of the OH^- and PO_4^{3-} group bands suggests that the basic apatite structure of the sample is not affected by the calcination.
- SEM micrograph of synthetic HA powder treated at 200°C and 800°C revealed particle morphology with dense and cloudy surface while the micrograph of natural HA powder extracted from bovine bone shows particle morphology of porous (voids found between particles) and smoother surfaces and a regular spherical shape.

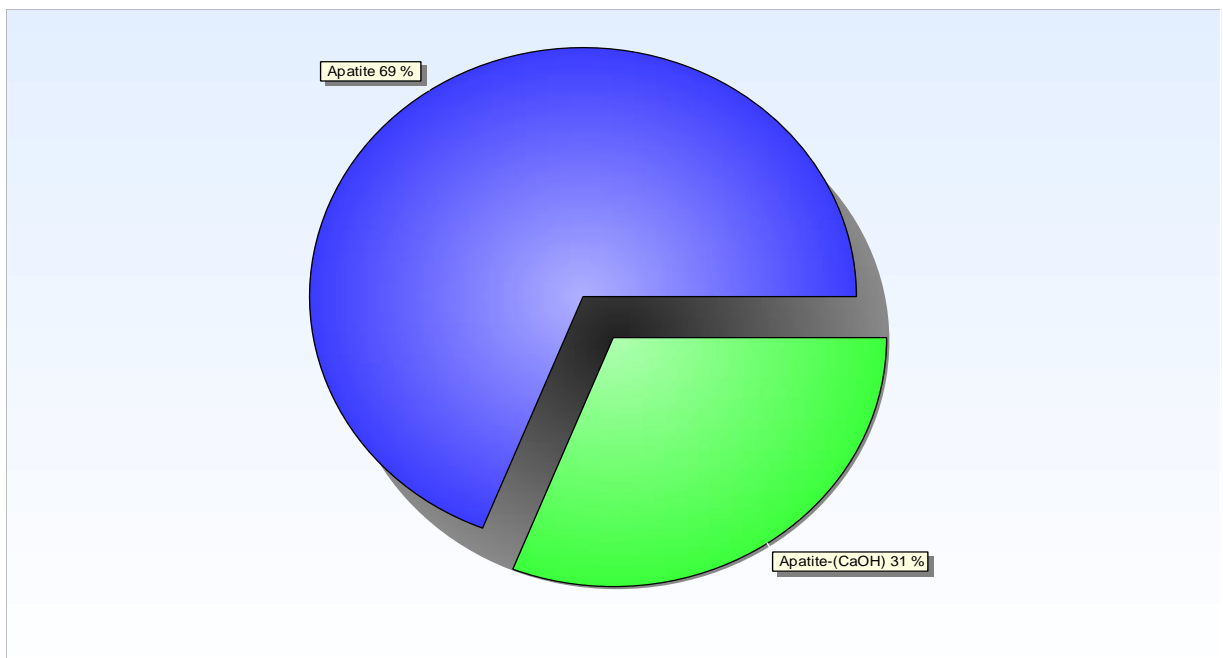
- The energy dispersive spectra show that whatever the composition studied, the elements: calcium (Ca) and phosphorus (P) are detected. The intensity of the calcium peak is always higher than that of the phosphorus peak. EDX confirms the results obtained by XRD (the existence of two structural forms HA and HA-CaOH).

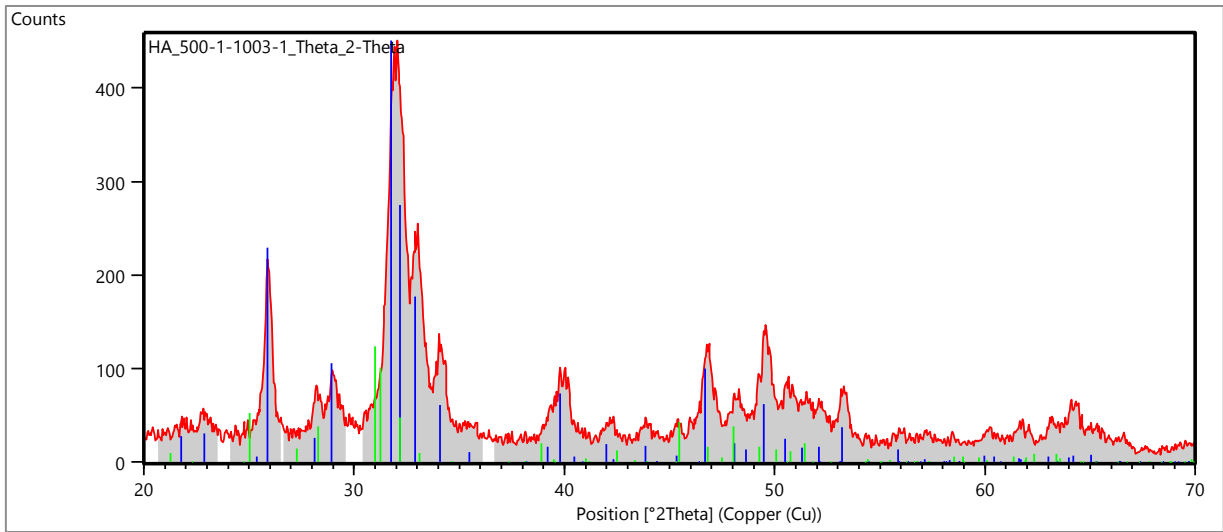
For future research, this work deserves to be continued and deepened in several directions. In addition to the influence of the heat-treatment temperature, factors such as pH, aging time, and drop rate should also be taken in consideration. In term of investigations, the study of the mechanical performances, and conducting in vitro tests using SBF solution, will help to determine hydroxyapatite qualification in terms of strength and bioactivity which is vital in deciding the suitability of applying HA in the biomedical field.

Appendix

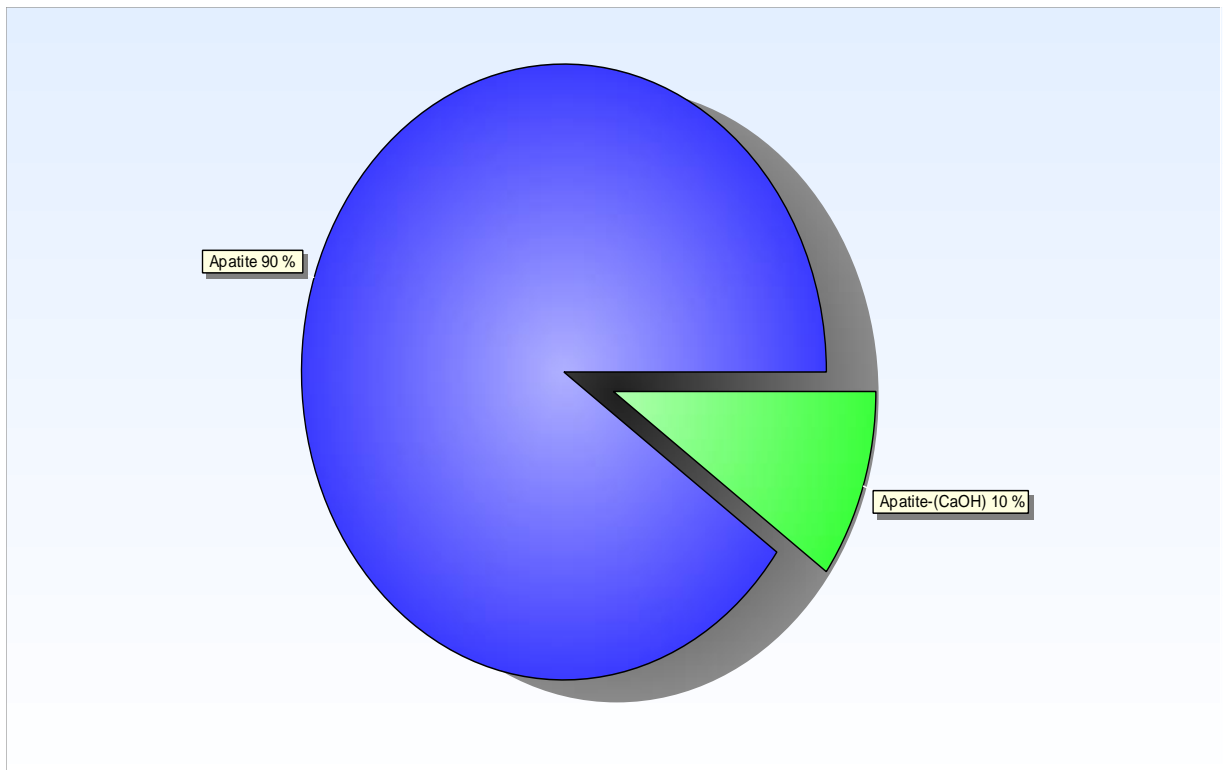


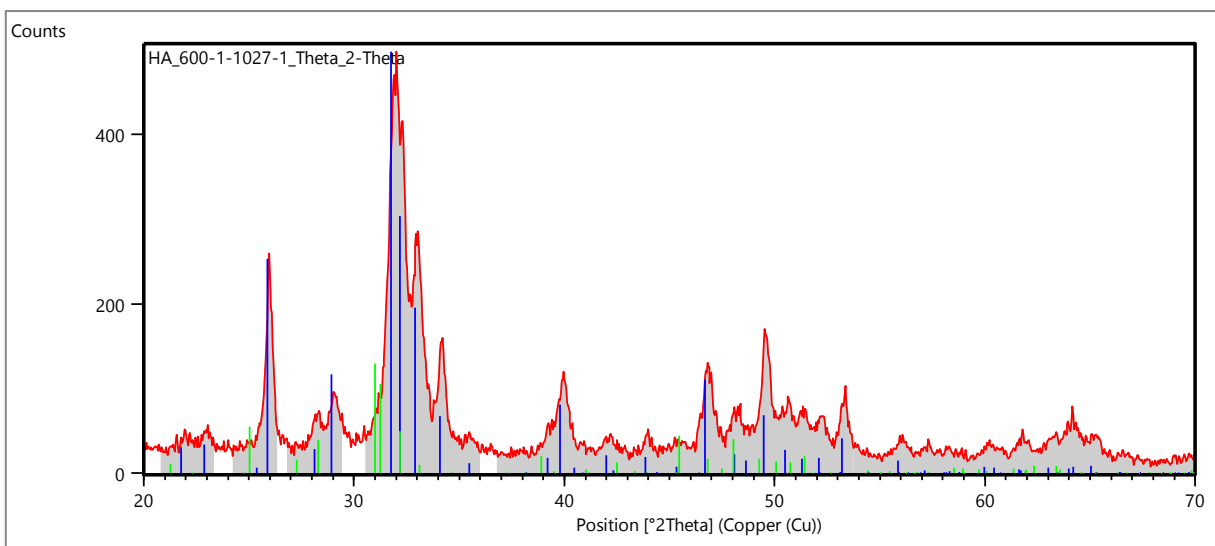
XRD of synthetic HA calcined at 200°C



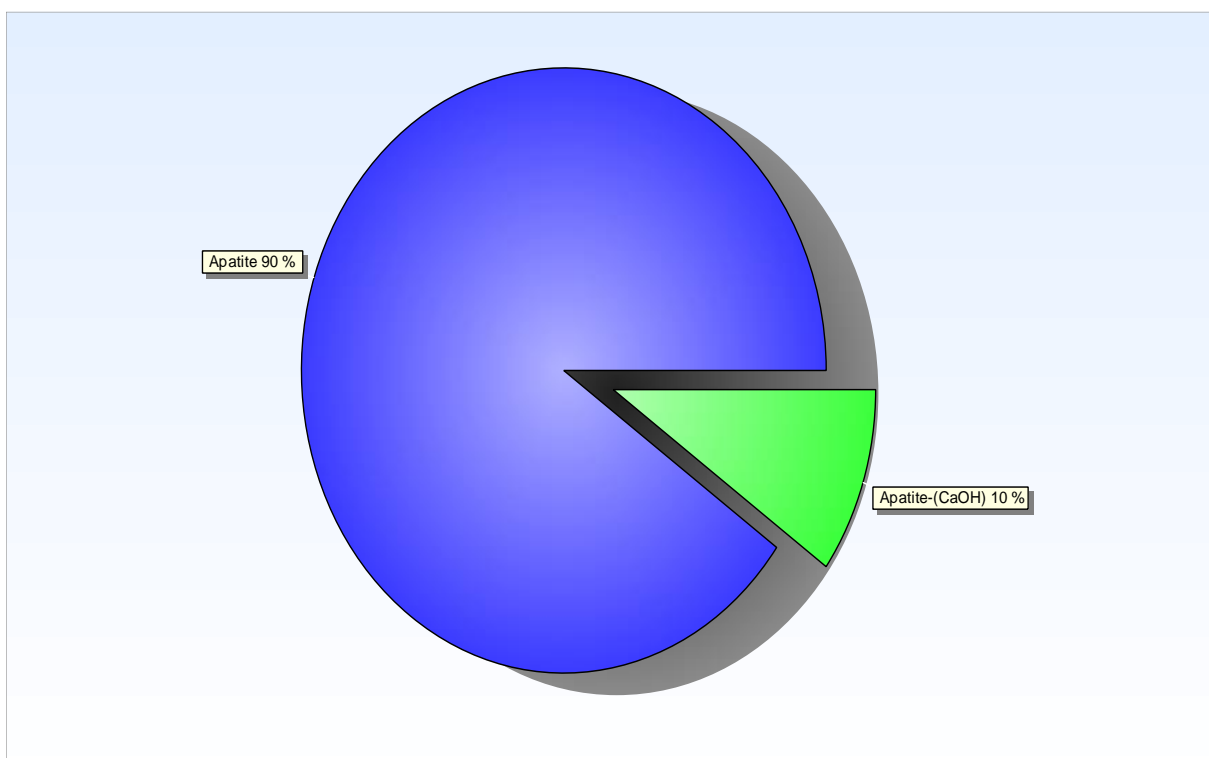


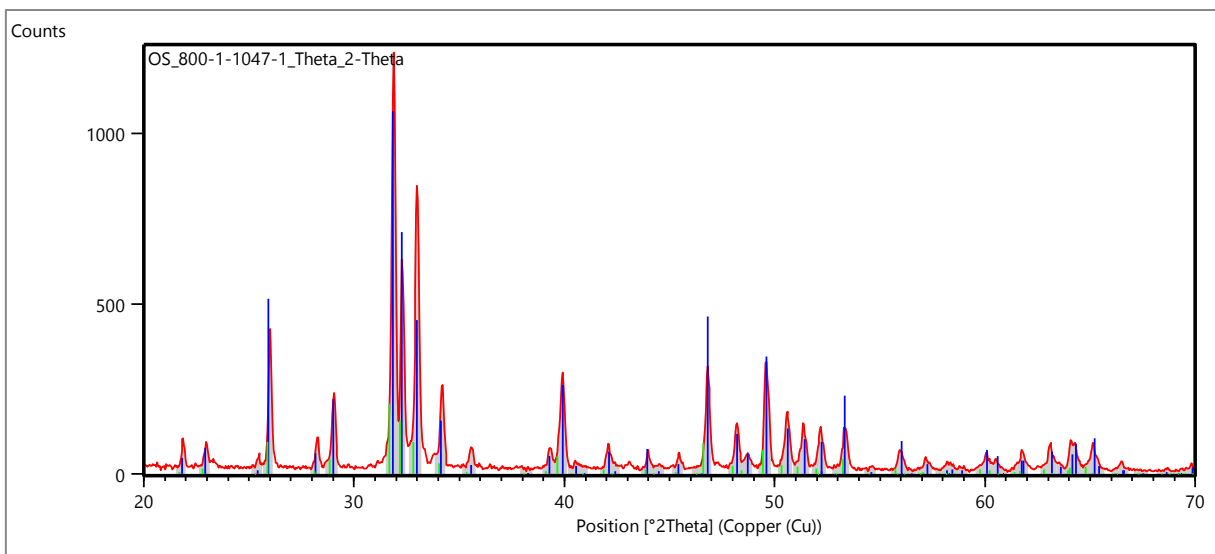
XRD of synthetic HA calcined at 500°C



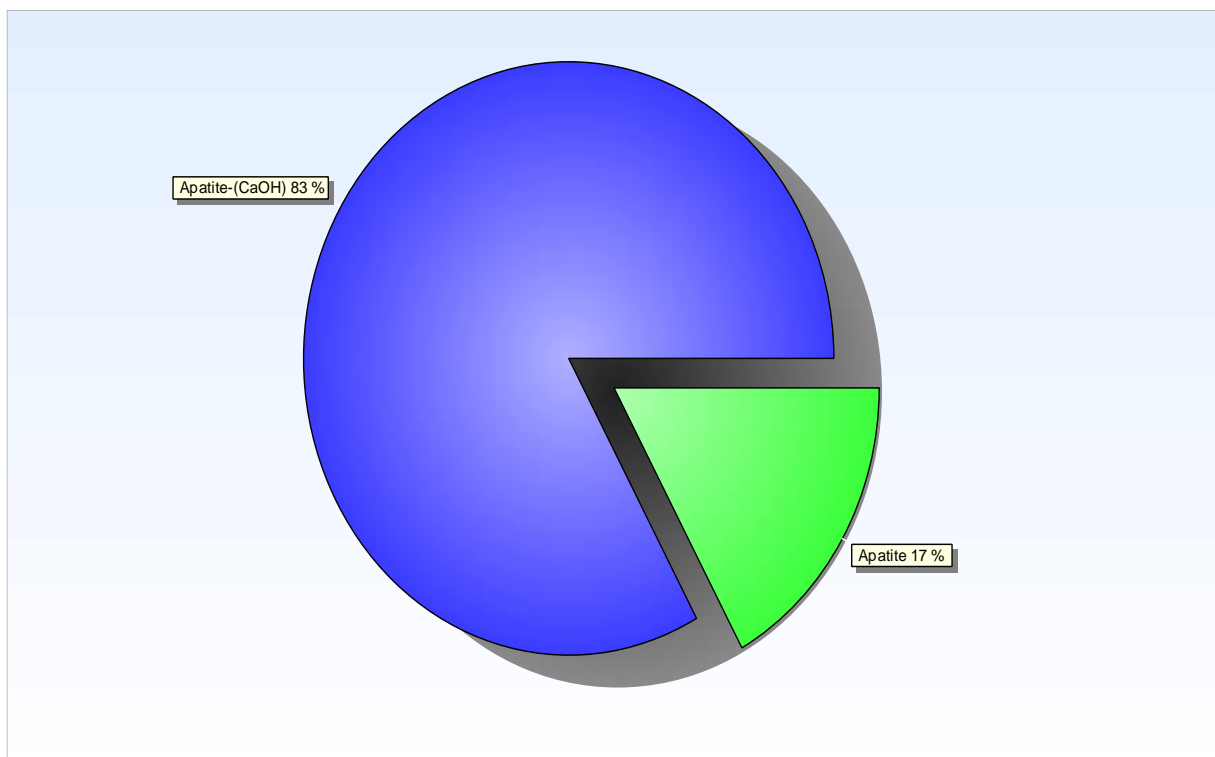


XRD of synthetic HA calcined at 600°C





XRD of natural HA extracted from bovine bone and calcined at 800°C



Name and formula

Reference code: 98-026-1063
Mineral name: Apatite
Compound name: Apatite
Common name: Apatite
Chemical formula: $H_2Ca_{10}O_{26}P_6$

Crystallographic parameters

Crystal system: Hexagonal
Space group: P 6₃/m
Space group number: 176

a (Å): 9,4190
b (Å): 9,4190
c (Å): 6,8810
Alpha (°): 90,0000
Beta (°): 90,0000
Gamma (°): 120,0000

Calculated density (g/cm³): 3,16
Volume of cell (10⁶ pm³): 528,68
Z: 1,00
RIR: 0,65

Subfiles and quality

Subfiles: User Inorganic
User Mineral
Quality: User From Structure (=)

Comments

Creation Date: 01/02/2011
Modification Date: 30/12/1899
Original ICSD space group: P6₃/M. IR, TGA, diffuse-reflectance spectroscopy. R = R(p).
The coordinates are those given in the paper but the atomic distances do not agree with those calculated during testing. The coordinates are probably correct.. At least one temperature factor is implausible or meaningless but agrees with the value given in the paper. X-ray diffraction (powder)
Structure type: Ca₅(PO₄)₃F. Temperature factors available

Temperature in Kelvin: 296
 Compound with mineral name: Apatite
 Structure type: $\text{Ca}_5(\text{PO}_4)_3\text{F}$
 Recording date: 2/1/2011
 ANX formula: A3B5X13
 Z: 1
 Calculated density: 3.16
 R value: 0.11
 Pearson code: hP44
 Wyckoff code: i h4 f e
 Structure TIDY: TRANS y,x,-z
 Publication title: Isomorphous substitutions of rare earth elements for calcium in synthetic hydroxyapatites
 ICSD collection code: 261063
 Structure: $\text{Ca}_5(\text{PO}_4)_3\text{F}$
 Chemical Name: Calcium Thulium Hexakis(phosphate) Hydroxide Oxide (9.8/0.2/6/1.8/0.2)
 Second Chemical Formula: $\text{Ca}_{10}(\text{P O}_4)_6(\text{O H})_2$

References

Structure: Lyashchenko, A.;Chebishev, A.;Chivireva, N.A.;Antonovich, V.P.;Marchenko, V.I.;Tkachenko, T.V.;Prisedsky, V.V.;Loboda, S.N.;Get'man, E.I.;Ardanova, L.I., *Inorganic Chemistry*, **49**, 10687 - 10693, (2010)

Peak list

No.	h	k	l	d [Å]	2Theta[deg]	I [%]
1	1	0	0	8,15709	10,837	20,3
2	1	0	1	5,25958	16,843	2,5
3	1	1	0	4,70950	18,828	3,9
4	2	0	0	4,07855	21,773	6,2
5	1	1	1	3,88640	22,864	6,9
6	2	0	1	3,50853	25,365	1,4
7	0	0	2	3,44050	25,875	50,8
8	1	0	2	3,17006	28,126	5,7
9	1	2	0	3,08309	28,937	23,4
10	1	2	1	2,81358	31,779	100,0
11	1	1	2	2,77813	32,195	60,9
12	0	3	0	2,71903	32,914	39,2
13	0	2	2	2,62979	34,065	13,5
14	3	0	1	2,52876	35,470	2,4
15	2	2	0	2,35475	38,189	0,2
16	1	2	2	2,29607	39,204	3,7
17	3	1	0	2,26237	39,813	16,4
18	2	2	1	2,22791	40,455	1,4
19	0	1	3	2,20804	40,835	0,1
20	3	1	1	2,14919	42,006	4,2
21	3	0	2	2,13326	42,334	0,7

Appendix

22	1	1	3	2,06210	43,869	3,9
23	0	4	0	2,03927	44,387	0,4
24	2	0	3	1,99921	45,325	1,5
25	0	4	1	1,95522	46,404	0,1
26	2	2	2	1,94320	46,708	22,3
27	3	1	2	1,89030	48,096	4,5
28	3	2	0	1,87137	48,614	3,0
29	1	2	3	1,84026	49,490	13,7
30	2	3	1	1,80578	50,501	5,5
31	4	1	0	1,78002	51,284	3,4
32	4	0	2	1,75427	52,093	3,6
33	3	0	3	1,75319	52,127	0,4
34	1	4	1	1,72330	53,102	0,3
35	0	0	4	1,72025	53,203	8,3
36	0	1	4	1,68323	54,469	0,3
37	2	3	2	1,64392	55,884	3,1
38	2	2	3	1,64304	55,916	0,0
- 39	0	5	0	1,63142	56,350	0,0
40	1	1	4	1,61583	56,943	0,0
41	3	1	3	1,61069	57,141	0,8
42	5	0	1	1,58741	58,058	0,3
43	2	0	4	1,58503	58,154	0,1
44	1	4	2	1,58096	58,318	0,5
45	3	3	0	1,56983	58,772	0,3
46	4	2	0	1,54155	59,959	1,6
47	3	3	1	1,53051	60,437	1,3
48	4	0	3	1,52402	60,721	0,0
49	4	2	1	1,50426	61,605	1,0
50	2	1	4	1,50223	61,697	0,8
51	5	0	2	1,47409	63,008	1,4
52	1	5	0	1,46506	63,442	0,4
53	0	3	4	1,45374	63,994	1,1
54	2	3	3	1,44999	64,179	1,6
55	1	5	1	1,43294	65,036	1,8
56	3	3	2	1,42819	65,279	0,4
57	2	4	2	1,40679	66,399	0,3
58	4	1	3	1,40624	66,429	0,2
59	2	2	4	1,38906	67,359	0,0
60	1	3	4	1,36935	68,462	0,1
61	0	6	0	1,35952	69,027	0,0
62	1	0	5	1,35702	69,172	0,0
63	1	5	2	1,34794	69,705	0,3
64	3	4	0	1,34102	70,117	0,1
65	0	6	1	1,33373	70,557	0,0
66	5	0	3	1,32943	70,820	0,0
67	1	1	5	1,32096	71,343	0,1
68	3	4	1	1,31625	71,637	0,6
69	4	0	4	1,31490	71,723	0,0
70	2	5	0	1,30618	72,276	0,5
71	0	2	5	1,30397	72,418	0,0
72	3	3	3	1,29547	72,970	0,1
73	2	5	1	1,28326	73,778	0,2
74	4	2	3	1,27943	74,036	0,5
75	3	2	4	1,26646	74,923	0,2
76	6	0	2	1,26438	75,068	0,1
77	1	2	5	1,25669	75,608	0,5
78	4	3	2	1,24946	76,123	0,3

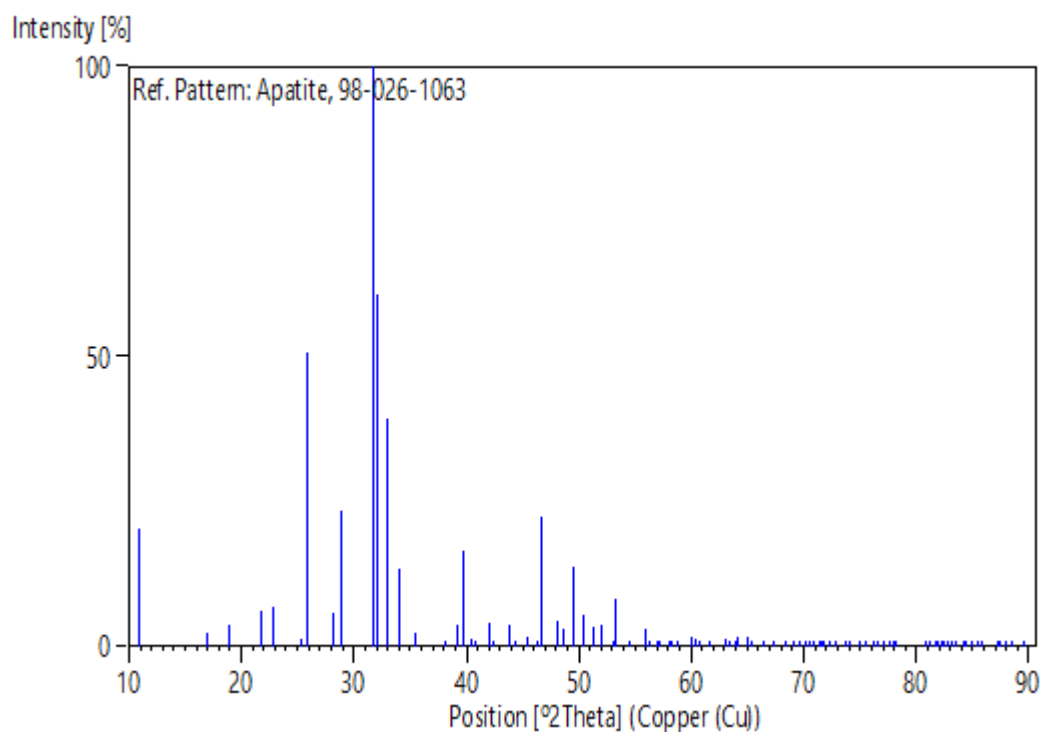
Appendix

79	1	6	0	1,24395	76,521	0,2
80	4	1	4	1,23699	77,030	0,4
81	1	5	3	1,23468	77,201	0,4
82	3	0	5	1,22788	77,708	0,0
83	6	1	1	1,22410	77,994	0,1
84	5	2	2	1,22114	78,219	0,7
85	2	2	5	1,18816	80,829	0,0
86	0	5	4	1,18375	81,193	0,0
87	4	4	0	1,17737	81,726	0,2
88	3	1	5	1,17575	81,863	0,0
89	6	1	2	1,16983	82,367	0,1
90	6	0	3	1,16951	82,394	0,0
91	5	3	0	1,16530	82,757	0,0
92	4	4	1	1,16051	83,175	0,1
93	3	3	4	1,15958	83,256	0,1
94	3	4	3	1,15767	83,424	0,3
95	3	5	1	1,14894	84,203	0,0
96	4	2	4	1,14804	84,284	0,2
97	0	0	6	1,14683	84,393	0,1
98	4	0	5	1,14074	84,949	0,0
99	1	0	6	1,13566	85,419	0,0
100	2	5	3	1,13504	85,477	0,1
101	6	2	0	1,13119	85,839	0,0
102	2	6	1	1,11620	87,277	0,0
103	1	5	4	1,11537	87,358	0,1
104	1	1	6	1,11427	87,467	0,3
105	4	4	2	1,11395	87,498	0,0
106	3	2	5	1,10868	88,021	0,1
107	0	2	6	1,10402	88,489	0,0
108	3	5	2	1,10371	88,521	0,2
109	6	1	3	1,09348	89,570	0,0

Structure

No.	Name	Elem.	X	Y	Z	Biso	sof	Wyck.
1	O1	O	0,00000	0,00000	0,18200	10,0000	0,5000	4e
2	O2	O	0,34640	0,08680	0,06140	10,0000	1,0000	12i
3	O3	O	0,58660	0,12230	0,25000	10,0000	1,0000	6h
4	O4	O	0,16370	0,48950	0,25000	10,0000	1,0000	6h
5	P1	P	0,39910	0,02960	0,25000	10,0000	1,0000	6h
6	CA1	Ca	0,24630	0,25420	0,25000	10,0000	1,0000	6h
7	CA2	Ca	0,33333	0,66667	0,00300	10,0000	1,0000	4f

Stick Pattern



Name and formula

Reference code: 98-015-0687
 Mineral name: Apatite-(CaOH)
 Compound name: Apatite-(CaOH)
 Common name: Apatite-(CaOH)
 Chemical formula: $H_{4.6}Ca_{9.63}O_{26.54}P_{5.78}$

Crystallographic parameters

Crystal system: Hexagonal
 Space group: P 6₃/m
 Space group number: 176
 a (Å): 9,4700
 b (Å): 9,4700
 c (Å): 6,8840
 Alpha (°): 90,0000
 Beta (°): 90,0000
 Gamma (°): 120,0000

Calculated density (g/cm³): 3,09
Volume of cell (10⁶ pm³): 534,65
Z: 1,00
RIR: 1,05

Subfiles and quality

Subfiles: User Inorganic
User Mineral
Quality: User From Structure (=)

Comments

Creation Date: 01/04/2006
Modification Date: 01/08/2008
Original ICSD space group: P6₃/M. Deviation from hydroxylapatite stoichiometry interpreted as incorporation of (HCO₂)⁽⁻⁾ formiate ions. The coordinates are those given in the paper but the atomic distances do not agree with those calculated during testing. The coordinates are probably correct. A site occupation is implausible or meaningless but agrees with the paper. At least one temperature factor missing in the paper. X-ray diffraction (powder)

Structure type: Ca₅(PO₄)₃(OH)_{1+x}. Rietveld profile refinement applied
The structure has been assigned a PDF number (calculated powder diffraction data): 01-073-2657

Compound with mineral name: Apatite-(CaOH)
Structure type: Ca₅(PO₄)₃(OH)_{1+x}
Recording date: 4/1/2006
Modification date: 8/1/2008
Mineral origin: synthetic
ANX formula: A6B10X27
Z: 1
Calculated density: 3.09
R value: 0.0708
Pearson code: hP47
Wyckoff code: i h4 f e

Structure TIDY: TRANS y,x,-z

Publication title: Formate incorporation in the structure of Ca-deficient apatite: Rietveld structure refinement

ICSD collection code: 150687

Structure: Ca₅(PO₄)₃(OH)_{1+x}

Chemical Name: Calcium Hydrogen Phosphate(V) Hydroxide Hydrate
(9.63/0.12/5.78/2.36/1.06)

Second Chemical Formula: $\text{Ca}_{9.63}(\text{PO}_4)_{5.78}(\text{OH})_{2.36}(\text{H}_2\text{O})_{1.06} \cdot \text{H}_0.12$

References

Structure: Dowker, S.E.P.; Elliott, J.C.; Wilson, R.M., *Journal of Solid State Chemistry*, **174**, 132-140, (2003)

Peak list

No.	h	k	l	d [Å]	2Theta[deg]	I [%]
1	1	0	0	8,20126	10,779	12,0
2	0	1	1	5,27271	16,801	2,3
3	1	1	0	4,73500	18,725	1,8
4	0	2	0	4,10063	21,655	3,0
5	1	1	1	3,90124	22,776	11,3
6	2	0	1	3,52296	25,260	1,4
7	0	0	2	3,44200	25,864	47,2
8	1	0	2	3,17381	28,092	5,5
9	1	2	0	3,09979	28,778	22,4
10	1	2	1	2,82646	31,630	100,0
11	1	1	2	2,78413	32,124	71,6
12	0	3	0	2,73375	32,732	49,0
13	0	2	2	2,63636	33,977	18,6
14	0	3	1	2,54074	35,297	2,8
15	2	2	0	2,36750	37,975	0,7
16	1	2	2	2,30339	39,075	6,0
17	3	1	0	2,27462	39,589	27,6
18	2	2	1	2,23880	40,250	1,8
19	1	0	3	2,20980	40,801	0,2
20	3	1	1	2,15977	41,790	7,1
21	3	0	2	2,14071	42,180	1,3
22	1	1	3	2,06496	43,806	7,3
23	0	4	0	2,05032	44,135	0,7
24	2	0	3	2,00246	45,247	3,0
25	4	0	1	1,96501	46,159	0,1
26	2	2	2	1,95062	46,519	44,2
27	3	1	2	1,89768	47,897	12,2
28	3	2	0	1,88150	48,335	6,3
29	1	2	3	1,84431	49,374	34,0
30	2	3	1	1,81493	50,228	12,9
31	4	1	0	1,78966	50,988	9,8
32	0	4	2	1,76148	51,864	8,8
33	0	3	3	1,75757	51,988	0,9
34	1	4	1	1,73209	52,811	0,7
35	0	0	4	1,72100	53,178	21,6
36	1	0	4	1,68431	54,431	1,3
37	2	3	2	1,65094	55,625	9,6
38	2	2	3	1,64772	55,744	0,1
39	0	5	0	1,64025	56,020	0,0
40	1	1	4	1,61747	56,880	0,2
41	1	3	3	1,61544	56,958	4,0
42	5	0	1	1,59558	57,733	1,6

Appendix

43	1	4	2	1,58785	58,041	1,6
44	0	2	4	1,58691	58,079	0,2
45	3	3	0	1,57833	58,425	2,1
46	4	2	0	1,54989	59,604	7,7
47	3	3	1	1,53842	60,094	5,2
48	4	0	3	1,52891	60,507	0,0
49	4	2	1	1,51204	61,253	3,3
50	2	1	4	1,50465	61,587	5,4
51	5	0	2	1,48072	62,694	6,8
52	1	5	0	1,47299	63,061	2,2
53	0	3	4	1,45643	63,862	5,5
54	2	3	3	1,45494	63,935	9,6
55	1	5	1	1,44039	64,659	11,5
56	3	3	2	1,43469	64,947	2,1
57	2	4	2	1,41323	66,058	1,4
58	4	1	3	1,41121	66,165	1,1
59	2	2	4	1,39206	67,194	0,0
60	1	3	4	1,37243	68,287	0,7
61	6	0	0	1,36688	68,603	0,3
62	1	0	5	1,35780	69,126	0,0
63	5	1	2	1,35420	69,337	1,8
64	3	4	0	1,34828	69,685	0,3
65	6	0	1	1,34070	70,136	0,1
66	0	5	3	1,33440	70,517	0,2
67	3	4	1	1,32314	71,207	5,9
68	1	1	5	1,32205	71,275	0,6
69	0	4	4	1,31818	71,517	0,1
70	2	5	0	1,31325	71,826	5,1
71	0	2	5	1,30520	72,339	0,2
72	3	3	3	1,30041	72,648	0,3
73	2	5	1	1,28999	73,330	2,1
74	4	2	3	1,28437	73,704	5,9
75	6	0	2	1,27037	74,653	1,0
76	3	2	4	1,26989	74,687	2,2
77	1	2	5	1,25827	75,496	5,6
78	4	3	2	1,25540	75,699	4,5
79	1	6	0	1,25068	76,035	2,1
80	4	1	4	1,24049	76,773	5,2
81	1	5	3	1,23958	76,840	6,7
82	6	1	1	1,23054	77,509	0,6
83	3	0	5	1,22966	77,575	0,1
84	5	2	2	1,22698	77,776	9,4
85	2	2	5	1,19018	80,664	0,4
86	5	0	4	1,18735	80,895	0,3
87	4	4	0	1,18375	81,193	3,2
88	3	1	5	1,17784	81,687	0,8
89	6	1	2	1,17549	81,885	1,0
90	6	0	3	1,17432	81,984	0,0
91	5	3	0	1,17161	82,215	0,7
92	4	4	1	1,16663	82,642	1,8
93	3	3	4	1,16322	82,938	1,5
94	3	4	3	1,16247	83,004	6,1
95	3	5	1	1,15500	83,661	0,1
96	4	2	4	1,15170	83,955	4,5
97	0	0	6	1,14733	84,348	2,4
98	0	4	5	1,14301	84,741	0,0
99	2	5	3	1,13979	85,037	1,7

Appendix

100	6	2	0	1,13731	85,266	0,3
101	0	1	6	1,13627	85,363	0,1
102	2	6	1	1,12210	86,704	0,0
103	4	4	2	1,11940	86,966	0,4
104	1	5	4	1,11907	86,998	4,3
105	1	1	6	1,11507	87,389	8,0
106	3	2	5	1,11109	87,781	2,5
107	5	3	2	1,10912	87,977	5,4
108	2	0	6	1,10490	88,400	0,1
109	6	1	3	1,09816	89,086	0,5
110	1	4	5	1,09124	89,803	0,1

Structure

No.	Name	Elem.	X	Y	Z	Biso	sof	Wyck.
1	O1	O	0,00000	0,00000	0,18080	0,5000	0,5900	4e
2	O2	O	0,34230	0,08220	0,07080	0,5000	0,9880	12i
3	O3	O	0,58050	0,11930	0,25000	0,5000	1,0000	6h
4	O4	O	0,15520	0,48780	0,25000	0,5000	0,9920	6h
5	P1	P	0,39860	0,02900	0,25000	0,5000	0,9630	6h
6	CA1	Ca	0,24740	0,25560	0,25000	0,5000	0,9380	6h
7	CA2	Ca	0,33333	0,66667	0,00200	0,5000	1,0000	4f

Stick Pattern

